



# Provenance of the Proterozoic Thelon Basin, Nunavut, Canada, from detrital zircon geochronology and detrital quartz oxygen isotopes

Sarah E. Palmer<sup>a,\*</sup>, T. Kurt Kyser<sup>a</sup>, Eric E. Hiatt<sup>b</sup>

<sup>a</sup> Department of Geological Sciences and Engineering, Queen's University, Kingston, Ont., Canada K7L 3N6

<sup>b</sup> Geology Department, University of Wisconsin Oshkosh, 800 Algoma Boulevard, Oshkosh, WI 54901, USA

Received 12 February 2003; accepted 7 October 2003

## Abstract

The Paleoproterozoic Thelon Basin in Nunavut, Canada, is one of several large quartz-dominated sedimentary basins developed on Paleoproterozoic and Archean rocks of the Canadian Shield. Coarse-grained quartz to sub-feldspathic sandstones and conglomerates of the Thelon Formation comprise the basin fill. Detrital zircons from the Thelon Formation have LAM-ICP-MS <sup>207</sup>Pb–<sup>206</sup>Pb ages ranging from 3.94 to 1.78 Ga, but most are Neoproterozoic (2.70–2.50 Ga). The  $\delta^{18}\text{O}$  values of quartz range from 7.7 to 13.9‰, and are typically 10–12‰. Ages, U/Zr ratios, and oxygen isotopic compositions of detrital quartz are consistent with a predominantly Neoproterozoic metasedimentary source, such as surrounds the eastern Thelon Basin and comprises the bulk of basement rocks within the Rae domain.

The three stratigraphic sequences of the Thelon Formation have  $\delta^{18}\text{O}$  ranges for detrital quartz and zircon ages that further constrain the source areas and support previous sequence-stratigraphic interpretations. The lower sequence contains reworked siltstone and sandstone clasts and 2.50–1.85 Ga zircons indicating a contribution from Paleoproterozoic terranes. Detrital quartz  $\delta^{18}\text{O}$  values range from 9.8 to 13.9‰, indicating a metamorphic source also, which is consistent with a proximal source for the lower sequence. The middle sequence contains zircons exhibiting the widest range of ages (3.94–1.78 Ga). A >3.4 Ga Neoproterozoic zircon population, cannot be correlated to the immediately surrounding basement and therefore indicates a distal source, possibly in the order of 1000–2000 km away. The upper sequence contains relatively few zircons due to extensive alteration but ages are predominantly early Paleoproterozoic and Neoproterozoic. The upper sequence strata contain the lowest  $\delta^{18}\text{O}$  values of quartz, indicating an influx of granitic material late in the depositional history of the basin. The geochronology and geochemistry of detrital grains within the Thelon Formation indicate that the source areas evolved from predominantly proximal to distal, and back to proximal as the basin filled.

© 2003 Elsevier B.V. All rights reserved.

**Keywords:** Zircons; <sup>207</sup>Pb–<sup>206</sup>Pb dating; Oxygen isotopes; Provenance; Paleoproterozoic; Thelon Basin

## 1. Introduction

The Thelon Basin is a large quartz arenite-dominated Paleoproterozoic intracratonic basin that unconform-

ably overlies older Paleoproterozoic and Archean basement rocks of the Rae domain in the Canadian Shield (Fig. 1). The basin is a target for unconformity-type uranium and base metal deposits formed through mixing of circulating basinal brines with basement fluids or rocks (e.g. Kotzer and Kyser, 1995; Kyser et al., 2000; Renac et al., 2002). The western Thelon

\* Corresponding author. Fax: +1-613-533-6592.

E-mail address: [Palmer@students.geol.queensu.ca](mailto:Palmer@students.geol.queensu.ca) (S.E. Palmer).

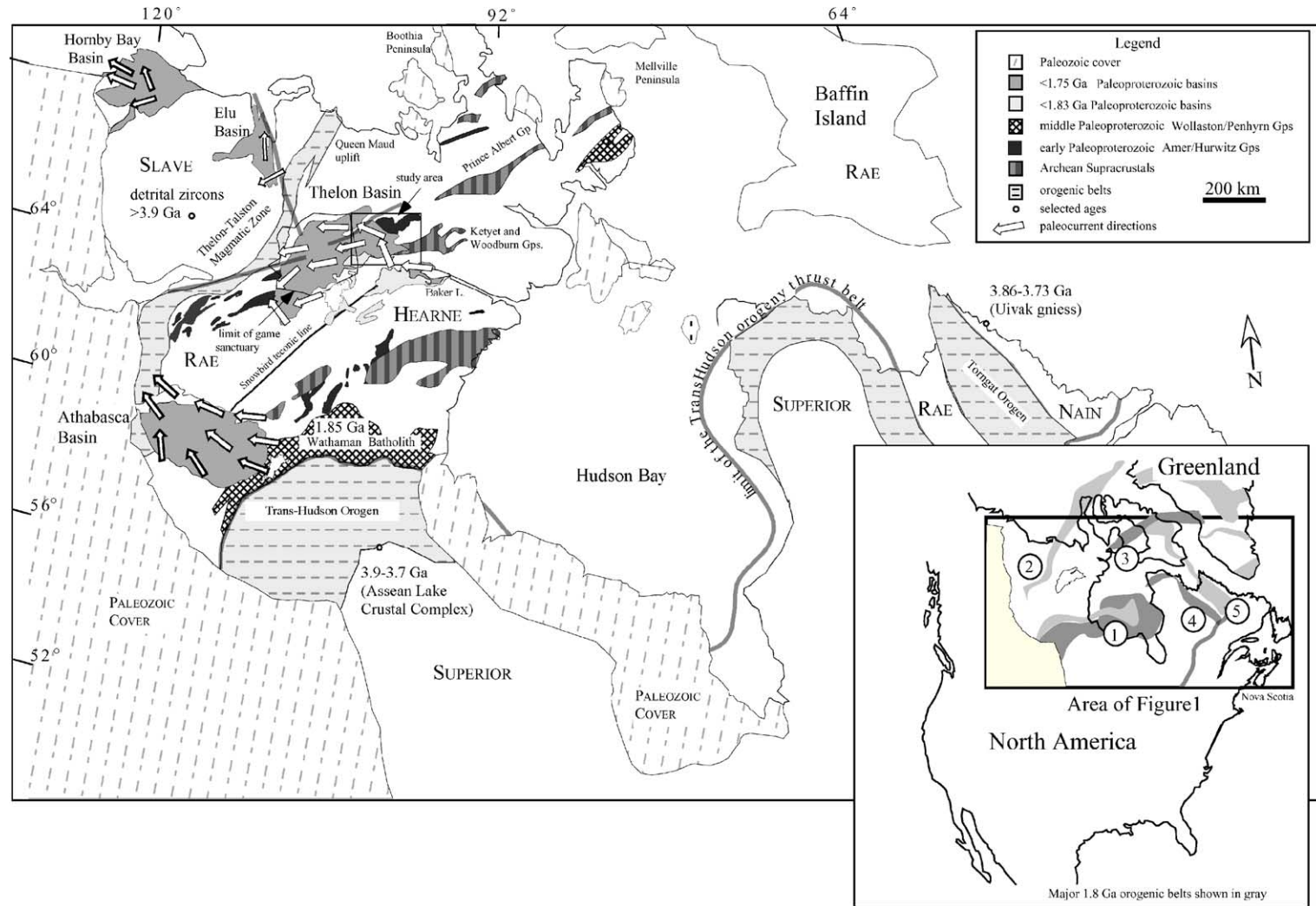


Fig. 1. Regional geology of the Canadian Shield showing Paleoproterozoic and Archean supracrustal successions and major tectonic assemblages surrounding the Rae-Hearne paleoplatform (modified after Wheeler et al., 1996; Aspler and Chiarenzelli, 1996). Ages of granitic plutons and Paleoproterozoic basement are indicated. Arrows represent paleocurrent directions after Fraser et al. (1970) in Paleoproterozoic supracrustal rocks of the Thelon Formation or time equivalents. The inset indicates major orogenic belts (dark gray) and continental magmatic arcs (light gray) of the ca. 1.8–2.0 Ga pan-continental orogenic events that sutured Archean cratons: (1) Trans-Hudson orogen, (2) Thelon–Talston magmatic zone (3) Foxe River fold belt, (4) Cape Smith belt and New Quebec orogen (probably a continuation of the Trans-Hudson) and (5) Torngat Orogen.

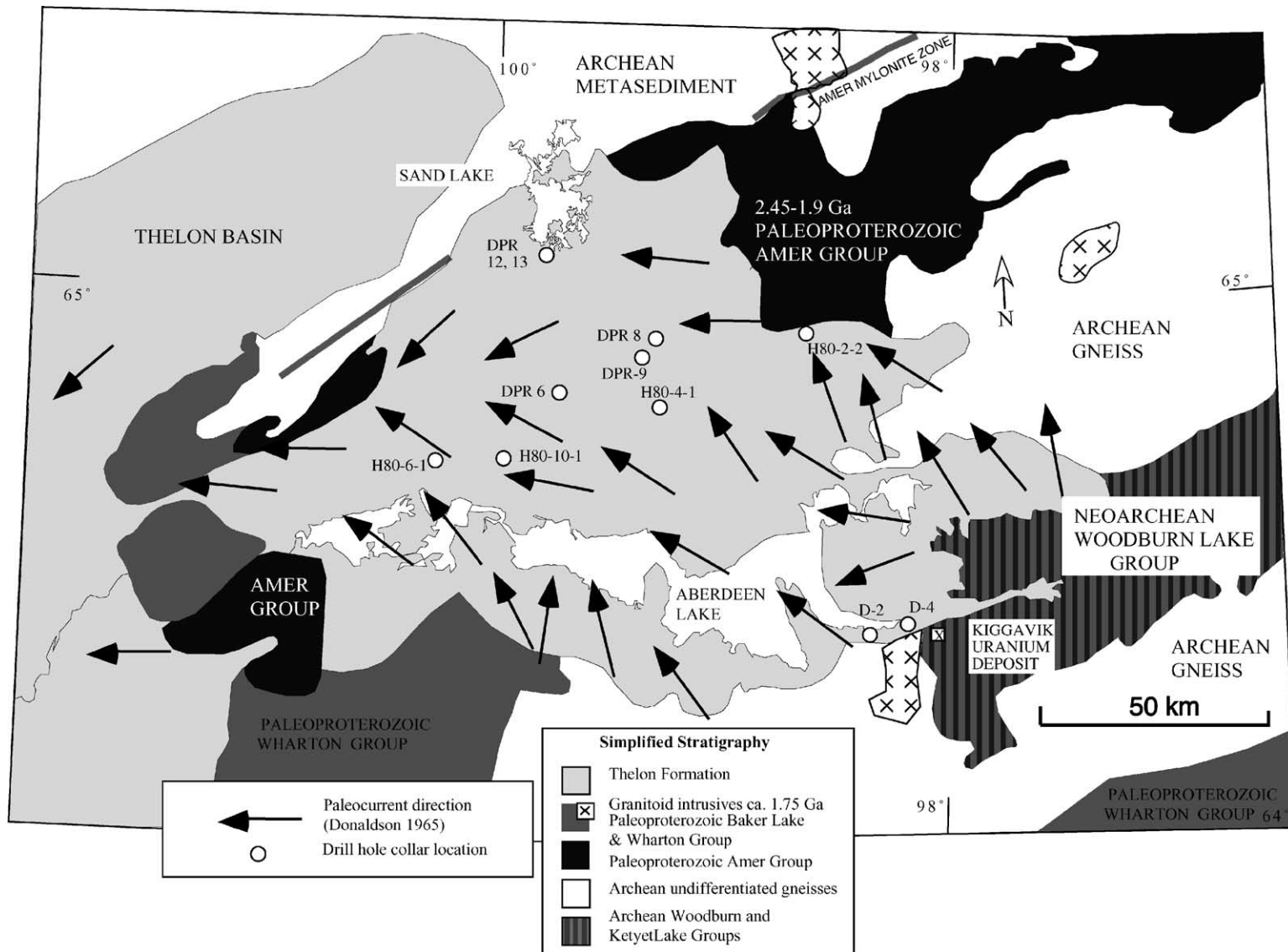


Fig. 2. Geology of the eastern Thelon Basin and surrounding basement rocks showing paleocurrent directions from Donaldson (1965). Drill hole locations and key outcrop exposures are shown as circles (sampled for zircons and quartz) and squares (sampled for quartz).

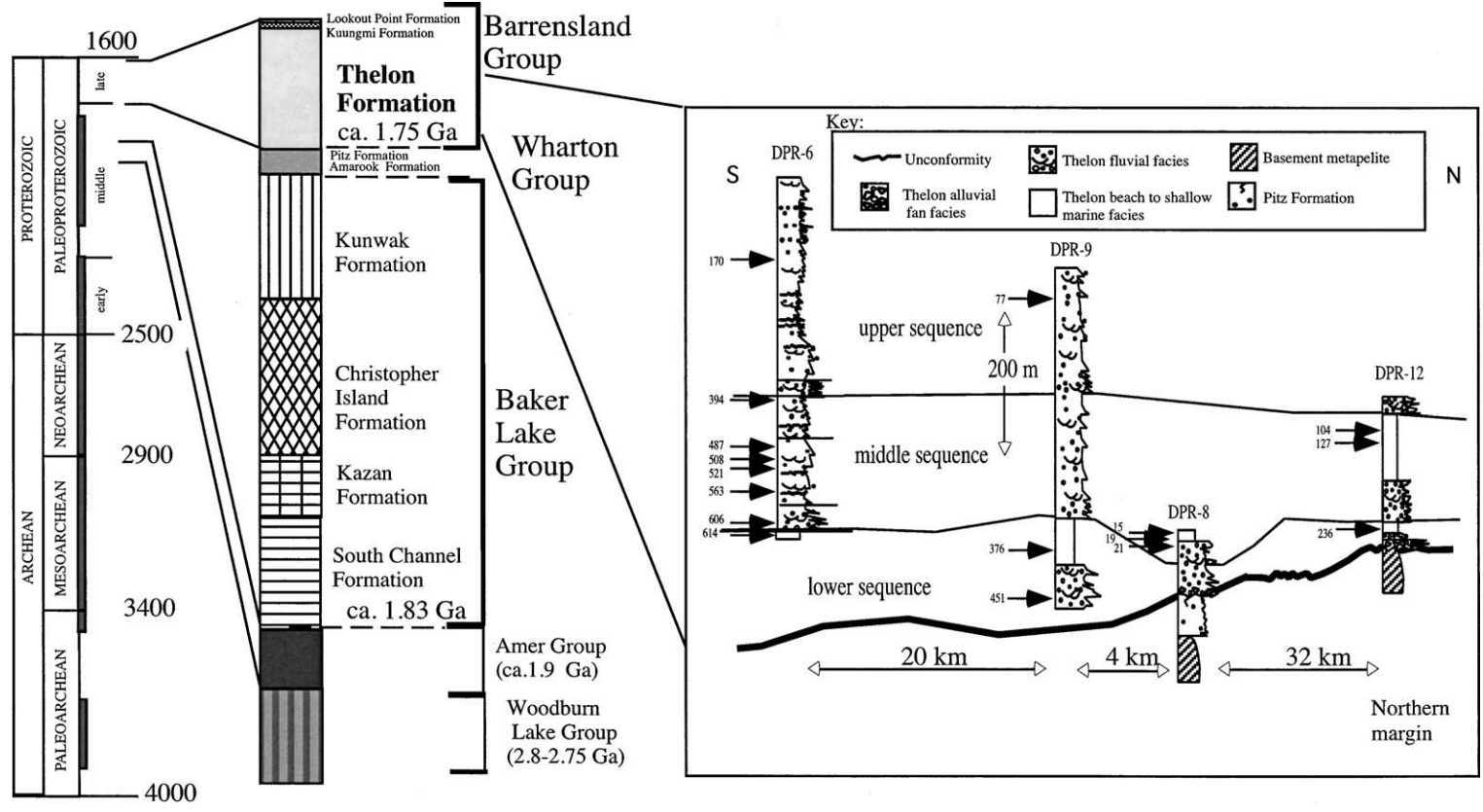


Fig. 3. Stratigraphic succession of basement underlying the Thelon Basin (after Gall et al., 1992). The Precambrian time scale (after Okulitch, 1999) includes dark boxes that indicate the distribution of ages from detrital zircons in the eastern Thelon Basin. Stratigraphy of the eastern Thelon Basin indicating three sequence-stratigraphic divisions of Hiatt et al. (1999) and Hiatt et al. (2003) and locations of sampled horizons (arrows) including depths (m) are also shown.

Basin is protected as part of the Thelon Game Sanctuary (Fig. 1) and therefore inaccessible for study. Exploration drill holes transect the northeast corner of the basin (Fig. 2), herein termed the eastern Thelon Basin, and provide an excellent cross-section through the preserved stratigraphy (Fig. 3).

The eastern Thelon Basin contains predominantly fluvial and nearshore quartz arenites and conglomerates of the Thelon Formation, the lowest unit in the Barrenland Group (Gall et al., 1992). Detailed stratigraphic sections (Fig. 3), interpreted by Hiatt et al. (2003), indicate that the Thelon Formation records three transgressive–regressive cycles, informally termed the lower, middle and upper sequences. Intense leaching of hematite, replacement of detrital feldspar, and other mineralogical changes observed in various stratigraphic intervals indicate these sediments have experienced substantial diagenesis (Renac et al., 2002), which altered the bulk composition of the rock making conventional source evaluation difficult. Currently, source area evaluation for the Thelon Formation rests on paleocurrent studies (Donaldson, 1965; Fraser et al., 1970; Jackson et al., 1984; Gall et al., 1992; Rainbird and Hadlari, 2000), which are good indicators of the general direction of paleo-drainage (Fig. 1). Many questions remain about nature and distance of sources, how they change through time, and the paleogeography of the basin.

The purpose of this paper is to use geochemical analysis of detrital material, specifically that material which is most resistant to later diagenesis and alteration, to indicate changes in provenance and the nature of the source areas. Changes in source can then be used to interpret the paleogeography and tectonic setting during the depositional history of the eastern Thelon Basin. The detrital assemblage is predominantly quartz (Donaldson, 1965; Gall et al., 1992) with minor lithic clasts and some well-preserved zircon, rutile and tourmaline. Intense alteration did not affect the geochemical nature of clasts such as quartz and zircon. Zircons are excellent province indicators as they occur in a wide variety of igneous and metamorphic rocks, and can survive transportation and diagenesis (Speer, 1980; Heaman and Parrish, 1991; Kroner et al., 2000). The age and geochemistry of zircons constrain the age and nature of the source rocks (Ross et al., 1992; Rainbird et al., 1997; Stewart et al., 2001; Cawood and Nemchin, 2001). Detrital quartz grains are ubiqu-

itous throughout the basin. Oxygen isotopic compositions combined with inclusion petrography of detrital quartz constrains the nature of the source region and indicates changes of provenance through time (cf. Vennemann et al., 1992). Herein, we use geochemical changes in detrital zircon and quartz populations in combination with petrography from defined stratigraphic intervals to evaluate provenance. The source terrane evaluations reflect the paleogeographic setting and paleotectonic evolution of the basin and its wider source region and support the sequence-stratigraphic interpretations by Hiatt et al. (2003).

## 2. Regional geology

The Thelon Basin is one of several Paleoproterozoic basins, including the Athabasca, Hornby and Elu (Fig. 1), that are found within the Canadian Shield. These basins are dominated by hematite-stained quartz arenites that are dominantly fluvial with minor shoreface and aeolian deposition. They were deposited in an intracratonic setting on well-developed paleosols and represent a period of relative tectonic stability. Most were preceded by thick accumulations of red-bed sedimentary and volcanic rocks deposited in fault-bounded basins in the foreland of major orogens (Ramaekers, 1981).

Regionally, paleocurrent directions (Fig. 1) indicate drainage was unimodal to the west in the Thelon Basin (Jackson et al., 1984; Gall et al., 1992). Fraser et al. (1970) suggested that the major continental drainage responsible for the Thelon Formation fed a basin to the west; Ramaekers (1981) interpreted that the regional slope decreased westward. A detailed study of paleocurrents in the eastern Thelon Basin (Fig. 2) indicated an overall westward direction of transport and supports the above interpretations. However, local variation in drainage such as north-directed paleocurrents at the southern margin (Donaldson, 1965) and unimodal transport towards the northwest (Rainbird and Hadlari, 2000) from the easternmost exposures of the Thelon Formation, near Baker Lake (Fig. 1) indicate a more complex depositional history.

The Thelon Basin lies unconformably on Paleoproterozoic and Archean supracrustal belts and plutonic rocks (Fig. 1). Basement includes Neoarchean supracrustals (Fig. 1) of the 2.96–2.71 Ga Woodburn

Lake and Ketyet Groups (Davis and Zaleski, 1998) to the east. These consist of metavolcanics, metapelite, calc-silicates, graphite schist, metagreywacke and banded iron formation. Similar rocks occur farther northeast of the Thelon Basin (Fig. 1) in the variably folded Prince Albert Group, which contains 2.8–2.75 Ga felsic volcanics (Schau, 1982). Neoarchean massive to weakly foliated granites dated at 2.61–2.59 Ga (LeCheminant and Roddick, 1991) surround the eastern Thelon Basin both to the north and south and underlie Paleoproterozoic supracrustals to the west of the study area. These granites contain accessory minerals of sphene, apatite, and zircon.

The 2.45–1.9 Ga Paleoproterozoic Amer Group (MacLachlan et al., 2000) metasediments crop out immediately northeast and southwest of the Thelon Basin (Fig. 1), and probably underlie much of it. The Amer Group metasediments occupy a large NE-trending synclinorium (Patterson, 1986) to the north of the eastern Thelon Basin (Fig. 2). The dominant lithologies are metamorphosed red-brown feldspathic siliciclastics, turbiditic mudstones, volcanics, carbonates, schist and orthoquartzite (LeCheminant et al., 1984). These rocks have been subjected to at least two periods of regional metamorphism and mineral assemblages indicate some units have reached middle amphibolite grade (Patterson, 1986).

The youngest supracrustals beneath the eastern Thelon Basin are the Paleoproterozoic Wharton and Baker Lake Groups (1.84–1.79 Ga; Rainbird et al., 2002), which occur exclusively to the south (Fig. 1). These comprise unmetamorphosed sedimentary rocks and felsic volcanic rocks, and unconformably overlie the Amer Group and Archean granitic gneiss (LeCheminant et al., 1983; Tella et al., 1985). The Baker Lake Group consists of red beds and alkaline intrusives, 1.85 Ga syenites and clastic rocks (Tella et al., 1985). The overlying Wharton Group includes 1.76 Ga siliceous rhyolite (LeCheminant et al., 1987) and feldspathic sandstones. Together the Wharton and Baker Lake Groups make up the lower Dubawnt Supergroup with a combined thickness of approximately 5 km (Gall et al., 1992). The Barrenland Group, which includes the Thelon Formation, makes up the upper part of the Dubawnt Supergroup.

The Wharton and Baker Lake Groups are coeval with at least two pulses of Paleoproterozoic (1.85–1.75 Ga) granitoid plutonism (Peterson et al.,

2000). Older granitoids (Fig. 2) are dominantly monzonites containing zircons and ferromagnesian minerals and were generated at the same time as minette volcanics of the Baker Lake Group. A later pulse of 1.76–1.75 Ga granitic rock is coeval with Wharton Group volcanism (Peterson et al., 2000) and includes a 1753 Ma fluorite-bearing granite (Loveridge et al., 1987) which underlies the Thelon Formation and constrains the onset of deposition within the eastern Thelon Basin (Miller et al., 1989). These later granites contain zircons which are euhedral and delicately zoned (Peterson et al., 2000).

Basement to the Dubawnt Supergroup was variably folded and metamorphosed by the ca. 1.92–1.69 Ga Trans-Hudson orogenic event to the south and the ca. 2.0–1.9 Ga Thelon–Talston orogen to the west (e.g. McNicoll et al., 2000). The Thelon–Talston orogen, produced by continental collision of the Slave Province into the western Churchill Province (Lucas et al., 1996), is analogous to the present day indentation of India into Asia (Molnar and Tapponnier, 1977) and probably produced large elevated plateaus (e.g. Queen Maud uplift, Fig. 1). Collision to the south at ca. 1.91–1.81 Ga between the western Churchill Province and the Superior Province resulted in the Trans-Hudson Orogen (Lucas et al., 1996) (Fig. 1) comprising extensive foreland fold and thrust belts of arc-related volcanic and plutonic rocks and volcanogenic clastic rocks (Hoffman, 1990). This orogenic belt is separated from the western Churchill Province by an extensive 1.85 Ga monzogranite–granodiorite batholith (Lewry et al., 1981).

### 3. Sedimentary petrology of the Thelon Formation

The sedimentology of the Thelon Formation, which is the oldest and thickest (1920 m) unit of the Barrenland Group (Gall et al., 1992), has been interpreted from numerous drill core samples (Fig. 2) and exposures in the eastern Thelon Basin (Hiatt et al., 2003). The eastern Thelon Basin presently consists of at least 650 m of strata dominated by braided fluvial facies, punctuated by aeolian and shoreface facies (Fig. 3).

Stratigraphic packaging based on detailed logging of drill core (Hiatt et al., 2003) indicates three

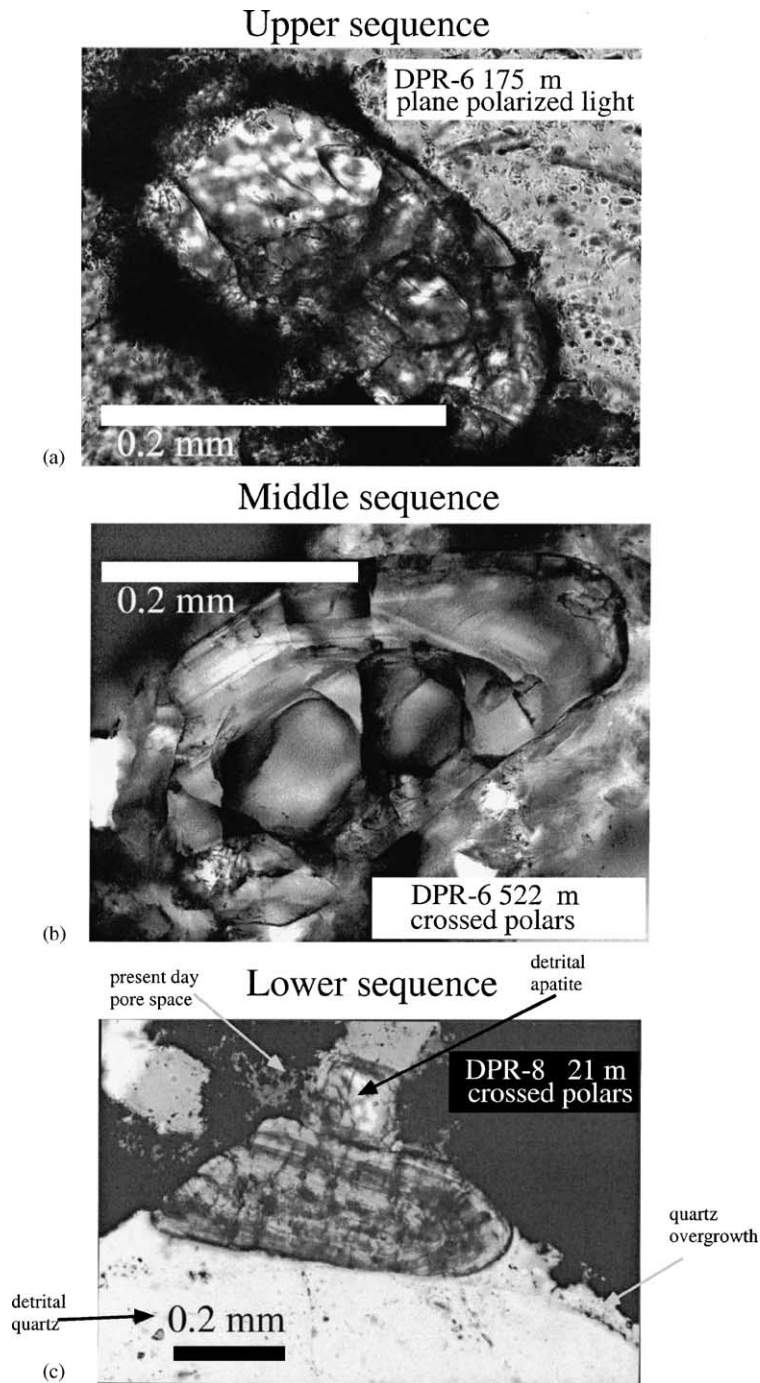


Fig. 4. Photomicrographs of (a) typical zoned zircon from the lower sequence which is armored by quartz overgrowths and shows no evidence of alteration. Also note detrital phosphate grain; (b) inclusion-bearing zircon from the middle sequence indicating clear non-metamict zircons with little alteration; and (c) rare preserved zircon from the upper sequence showing intense alteration.

depositional sequences, herein termed lower, middle and upper sequence (Fig. 3). The lower sequence rests unconformably on basement and is characterized by coarse-grained, poorly sorted, immature conglomerates, interpreted as alluvial fan to proximal braided stream deposits. This facies is overlain by fluvial facies containing variable amounts of clay and near shore facies of well-cemented quartz sand. Both facies contain detrital zircon and phosphate grains. Zircons are abundant in nearshore facies where they occur in 1–2 mm dark bands within sandy cross-laminated beds. The zircons are typically quartz-armored (Fig. 4a) and are uncorroded. Rounded zircons occur rarely in detrital quartz grains implying some reworking of sedimentary sources. In the fluvial facies, zircons were recovered from thin planar-laminated clay-rich sandstone and mudstone layers. Petrographic observations under crossed-polarized light indicate that some zircons have primary zoning (Fig. 4a).

The middle sequence is composed of sandstone in fining-upward packages that represent fluvial deposition in or near the center of the study area, and well-sorted nearshore facies strata at the basin margins. This sequence contains horizons that are extremely clay-rich and contain abundant stylolites. Quartz grains are often poorly preserved and embayed grain boundaries attest to intense dissolution. Muscovite, zircon and apatite are present both as mineral inclusions and as detrital grains. Zircons are inclusion-rich and commonly exhibit zoning or rounded overgrowths (Fig. 4b). Preserved banded iron formation clasts are observed in hand samples. Most lithic clasts, however, are highly altered or completely replaced by clay.

The base of the upper sequence is defined by a 10 m interval of very coarse-grained fluvial sandstones. The upper sequence is composed of fluvial facies only. The upper sequence is clay-rich and contains both authigenic carbonate and feldspar cements indicating that late stage diagenesis has affected these sediments (Renac et al., 2002). Quartz grains contain zircon and apatite inclusions as well as muscovite and tourmaline and possibly rutile, however, these minerals are not common as detrital grains (Fig. 4c). Chert and strained quartz with textures typical of metamorphic grains are also found in the upper sequence but are very altered.

## 4. Methodology

For this study we sampled several diamond drill holes in the eastern Thelon Basin (Fig. 2) that contained thick successions of Thelon Formation sandstones spanning the sequence boundaries (Fig. 3). Zircons selected from intervals rich in heavy minerals, were characterized by petrography prior to separation. Detrital quartz grains were selected from zircon-bearing samples and from typical sandstone horizons within each sequence. Petrography indicates a variety of quartz populations including monocrystalline grains, polycrystalline grains and chert. In the poorly sorted material, most of these quartz varieties occur in approximately equal abundance throughout the size range. Separates were obtained from crushed and sieved fractions using conventional handpicking, heavy liquid, and magnetic separation methods.

### 4.1. Laser-ablation microprobe inductively coupled plasma mass spectrometry (LAM-ICP-MS)

Zircon grains were concentrated by heavy liquid separation (tetrabromide, sp. gr. 2.96 at 20 °C), Frantz isodynamic magnetic separation, and handpicking under a binocular microscope, and were then mounted in FEP Teflon® sheets for analysis. All zircons sampled for this study are rounded to subrounded due to natural abrasion during sedimentary transport. Zircons were categorized based on color (clear, brown, orange or white) and size (Table 1).

Isotopic measurements on zircons were made by laser ablation with a LUV 266, New Wave-Merchanteck laser coupled to a Finigan MAT ELEMENT HR-ICP-MS. The laser was run for spot analysis with a pulse width of 50 µm, a fire rate of 2 Hz and an output of 2 mJ. Ablation pit diameters did not exceed 20 µ. Zircons were analyzed by ICP-MS for  $^{238}\text{U}$ ,  $^{235}\text{U}$ ,  $^{204}\text{Pb}$ ,  $^{206}\text{Pb}$ ,  $^{207}\text{Pb}$ , and  $^{208}\text{Pb}$ .  $^{204}\text{Pb}$  was corrected for  $^{204}\text{Hg}$  interference using  $^{202}\text{Hg}$ . The  $^{206}\text{Pb}/^{204}\text{Pb}$  ratios ranged from 0 to upwards of 1000 and averaged around 600. Ninety percent of the data were above 50 and, of the few analysis below 50, most also had low  $^{207}\text{Pb}$  counts. An in-house standard of Brownell zircons ( $1831 \pm 9$  Ma by thermal ionization mass spectrometry (TIMS; McNicoll et al., 1992) was used as an external standard. Analytical error is ~1% based on repeat measurement of the

Table 1  
 $^{207}\text{Pb}$ - $^{206}\text{Pb}$  ages and U/Zr ratios for detrital zircon populations

Analysis	$^{207}\text{Pb}$ - $^{206}\text{Pb}$	$^{207}\text{Pb}$ - $^{206}\text{Pb}$ age (Ma)	Error (Ma)	Morphology	Size (microns)	Color	$^{238}\text{U}/^{96}\text{Zr}$	Analysis	$^{207}\text{Pb}$ - $^{206}\text{Pb}$	$^{207}\text{Pb}$ - $^{206}\text{Pb}$ age (Ma)	Error (Ma)	Morphology	Size (microns)	Color	$^{238}\text{U}/^{96}\text{Zr}$
Upper sequence								Middle sequence							
6-170								6-508							
A	0.1563	2416	±17	r,i	200	b		B	0.1448	2285	±17	r,i	150	b	
A	0.1665	2523	±17	r,i	200	b		C	0.1125	1840	±17	r,i	200	w	
B	0.1154	1885	±20	r,eq	180	b		C	0.1120	1832	±18	r,i	200	w	
C	0.1606	2462	±17	c,eq	200	b		<b>D</b>	<b>0.1427</b>	<b>2260</b>	±17	<b>r,l</b>	<b>200</b>	<b>w</b>	
C	0.1676	2534	±17	c,eq	200	b		D	0.1422	2254	±17	r,l	200	w	
D	0.1589	2444	±17	r,eq	180	b		E	0.1985	2814	±16	r,l	200	w	
D	0.1586	2441	±17	r,eq	180	b		E	0.2037	2856	±16	r,l	200	w	
E	0.2065	2878	±17	s,i	200	b		F	0.1831	2681	±16	r,i	150	w	
E	0.2555	3219	±16	s,i	200	b		F	0.1846	2695	±16	r,i	150	w	
F	0.2439	3146	±15	r,eq	100	w		G	0.1965	2797	±17	r,eq	280	b	
F	0.2014	2837	±17	r,eq	100	w		G	0.2012	2836	±16	r,eq	280	b	
G	0.1826	2677	±16	s,l	200	w		G	0.1876	2721	±17	r,eq	280	b	
G	0.1897	2740	±16	s,l	200	w		H	0.1859	2706	±17	s,eq	280	b	
<b>H</b>	<b>0.2026</b>	<b>2847</b>	±16	<b>s,l</b>	<b>200</b>	<b>w</b>		<b>H</b>	<b>0.1881</b>	<b>2726</b>	±16	<b>s,eq</b>	<b>280</b>	<b>b</b>	
<b>H</b>	<b>0.1855</b>	<b>2703</b>	±16	<b>s,l</b>	<b>200</b>	<b>w</b>		6-521							
I	0.2294	3048	±16	s,eq	180	w		A	0.1829	2679	±16	r,eq	100	w	
I	0.2040	2859	±15	s,eq	180	w		A	0.1725	2582	±16	r,eq	100	w	
J	0.1850	2698	±17	e,l	200	b		B	0.1702	2560	±16	r,l	200	w	
6-394								B	0.1777	2632	±16	r,l	200	w	
<b>A</b>	<b>0.1933</b>	<b>2771</b>	±15	<b>c,eq</b>	<b>100</b>	<b>w</b>		B	0.1664	2522	±17	r,l	200	w	
<b>A</b>	<b>0.1772</b>	<b>2627</b>	±17	<b>c,eq</b>	<b>100</b>	<b>w</b>		C	0.1207	1967	±17	s,eq	200	b	
B	0.2872	3403	±15	e,eq	100	w		C	0.1086	1778	±16	s,eq	200	b	
B	0.1854	2702	±17	e,eq	100	w		D	0.1741	2597	±17	e,l	200	cl	
C	0.2975	3457	±16	r,eq	50	w		D	0.1474	2316	±17	e,l	200	cl	
Middle sequence								E	0.1987	2815	±17	s,l	400	w	
6-487								E	0.1931	2769	±16	s,l	400	w	
A	0.1601	2457	±16	r,eq	200	w		F	0.1750	2606	±17	s,l	500	b	
A	0.2274	3034	±16	r,eq	200	w		F	0.2266	3028	±17	s,l	500	b	
A	0.1482	2325	±18	r,eq	200	w		G	0.1478	2321	±17	r,eq	300	b	
B	0.1551	2403	±17	s,l	300	w		G	0.1942	2778	±16	r,eq	300	b	
B	0.1429	2263	±16	s,l	300	w		H	0.1804	2657	±16	r,l	200	w	
B	0.1593	2448	±17	s,l	300	w		H	0.1764	2619	±17	r,l	200	w	
<b>C</b>	<b>0.1589</b>	<b>2444</b>	±17	<b>s,eq</b>	<b>300</b>	<b>w</b>		I	0.1436	2271	±17	r,eq	100	w	
C	0.3355	3642	±16	s,eq	300	w		J	0.1865	2711	±17	r,l	180	w	
D	0.2074	2885	±17	r,eq	200	w		J	0.1839	2688	±16	r,l	180	w	
D	0.2059	2874	±16	r,eq	200	w		6-563							
6-489								<b>A</b>	<b>0.1577</b>	<b>2431</b>	±17	<b>s,l</b>	<b>150</b>		
A	0.3825	3841	±16	s,l	280	b		A	0.1772	2627	±17	s,l	150		
A	0.3633	3764	±15	s,l	280	b		A	0.1641	2498	±17	s,l	150		
A	0.2932	3409	±16	s,l	280	b		B	0.1408	2237	±17	r,eq	100		
B	0.2572	3229	±15	s,i	200	b		B	0.1455	2294	±17	r,eq	100		
B	0.1886	2731	±15	s,i	200	b		C	0.1509	2356	±17	r,eq	80		
C	0.1153	1885	±18	s,eq	100	b		C	0.2887	3410	±16	r,eq	80		
D	0.2884	3409	±16	s,eq	100	c		D	0.1973	2804	±16	r,l	150	w	

Table 1 (Continued)

Analysis	$^{207}\text{Pb}-^{206}\text{Pb}$	$^{207}\text{Pb}-^{206}\text{Pb}$ age (Ma)	Error (Ma)	Morphology	Size (microns)	Color	$^{238}\text{U}/^{96}\text{Zr}$	Analysis	$^{207}\text{Pb}-^{206}\text{Pb}$	$^{207}\text{Pb}-^{206}\text{Pb}$ age (Ma)	Error (Ma)	Morphology	Size (microns)	Color	$^{238}\text{U}/^{96}\text{Zr}$
6-508								D	0.1850	2698	±17	r,l	150	w	
A	0.1901	2743	±16	r,eq	200	w		E	0.2950	3444	±16	s,i	100	w	
A	0.1849	2697	±16	r,eq	200	w		<b>E</b>	<b>0.1746</b>	<b>2602</b>	<b>±16</b>	<b>s,i</b>	<b>100</b>	<b>w</b>	
Middle sequence								Middle sequence							
6-606								8-15							
A	0.1643	2500	±17	r,l	300	w		L	0.2135	2932	±16	r,eq	150	b	0.0007
<b>A</b>	<b>0.2595</b>	<b>3243</b>	<b>±16</b>	<b>r,l</b>	<b>300</b>	<b>w</b>		L	0.2107	2911	±16	r,eq	150	b	0.0007
B	0.4078	3938	±15	s,eq	300	b		8-19							
B	0.3518	3715	±15	s,eq	300	b		A	0.1335	2144	±17	r,eq	200	o	0.0011
<b>C</b>	<b>0.2034</b>	<b>2854</b>	<b>±15</b>	<b>r,eq</b>	100	<b>w</b>		A	0.1235	2008	±17	r,eq	200	o	0.0006
C	0.2099	2905	±16	r,eq	100	w		B	0.1294	2090	±17	s,l	300	cl	0.0005
<b>D</b>	<b>0.1582</b>	<b>2437</b>	<b>±17</b>	<b>s,l</b>	<b>350</b>	<b>o</b>		B	0.1285	2076	±18	s,l	300	cl	0.0004
<b>D</b>	<b>0.1628</b>	<b>2485</b>	<b>±16</b>	<b>s,l</b>	<b>350</b>	<b>o</b>		B	0.1182	1929	±18	s,l	300	cl	0.0004
E	0.1760	2616	±16	r,l	280	w		C	0.1861	2708	±17	r,eq	200	w	0.0005
E	0.1784	2638	±17	r,l	280	w		C	0.1962	2795	±17	r,eq	200	w	0.0005
F	0.1824	2675	±16	r,l	400	w		D	0.1946	2782	±15	r,l	250	cl	0.0005
F	0.1789	2643	±16	r,l	400	w		D	0.1998	2825	±16	r,l	250	cl	0.0009
<b>G</b>	<b>0.1650</b>	<b>2508</b>	<b>±17</b>	<b>s,i</b>	<b>300</b>	<b>w</b>		8-21							
G	0.1754	2610	±17	s,i	300	w		A	0.1942	2778	±16	r,l	150	b	0.0008
H	0.1624	2481	±16	c,l	280	b		A	0.1899	2741	±17	r,l	150	b	0.0005
H	0.1803	2656	±16	c,l	280	b		B	0.1735	2592	±16	e,l	250	b	0.0018
I	0.1673	2531	±17	c,l	150	cl		C	0.1762	2617	±17	r,l	250	b	0.0056
I	0.1968	2800	±16	c,l	150	cl		C	0.1787	2641	±16	r,l	250	b	0.0012
J	0.1700	2558	±16	c,l	100	w		D	0.1675	2533	±17	r,eq	200	b	0.0063
<b>J</b>	<b>0.1723</b>	<b>2580</b>	<b>±16</b>	<b>c,l</b>	<b>100</b>	<b>w</b>		E	0.1738	2595	±16	r,eq	250	b	0.0018
								F	0.1810	2662	±16	r,eq	250	b	0.0010
8-15								G	0.1638	2495	±17	r,eq	200	b	0.0029
A	0.2104	2909	±16	r,l	250	b	0.0018	H	0.1675	2533	±17	s,eq	250	b	0.0031
A	0.1695	2553	±16	r,l	250	b	0.0018	I	0.1609	2465	±17	r,eq	250	b	0.0040
A	0.2190	2973	±16	r,l	250	b	0.0021	12-104							
B	0.2915	3425	±16	s,l	300	w	0.0152	A	0.2229	3002	±15	r,eq	170	b	0.0057
B	0.2683	3296	±16	s,l	300	w	0.0047	A	0.2314	3062	±15	r,eq	170	b	0.0069
B	0.2538	3209	±15	s,l	300	w	0.0050	B	0.1710	2567	±17	r,eq	180	b	0.0010
C	0.2478	3171	±15	r,eq	100	b	0.0055	B	0.1702	2560	±16	r,eq	180	b	0.0010
C	0.2660	3282	±16	r,eq	100	b	0.0058	C	0.2164	2954	±17	r,eq	200	b	0.0041
D	0.2469	3165	±18	r,eq	150	w	0.0029	C	0.2295	3049	±16	r,eq	200	b	0.0044
D	0.2330	3073	±16	r,eq	150	w	0.0047	D	0.1873	2719	±16	r,eq	100	b	0.0023
E	0.1537	2388	±16	r,l	400	w	0.0012	E	0.2574	3231	±16	r,eq	200	b	0.0051
E	0.2733	3325	±15	r,l	400	w	0.0044	E	0.2652	3278	±16	r,eq	200	b	0.0048
F	0.1981	2811	±16	r,eq	200	w	0.0025	F	0.1430	2264	±17	r,eq	200	b	0.0020
F	0.1709	2566	±17	r,eq	200	w	0.0038	F	0.1501	2347	±17	r,eq	200	b	0.0023
G	0.2085	2894	±16	r,l	300	w	0.0024	G	0.1746	2602	±16	r,eq	220	b	0.0011
G	0.2128	2927	±16	r,l	300	w	0.0024	G	0.1767	2622	±17	r,eq	220	b	0.0012
G	0.2115	2917	±16	r,l	300	w	0.0032	G	0.1880	2725	±16	r,eq	220	b	0.0010



Brownell zircon. Because material is introduced into the mass spectrometer by laser ablation, the absolute value of each isotope is not measured as precisely as in other methods such as TIMS, which involves wet chemical preparation. Although LAM-ICP-MS lacks the  $\sim 0.1\%$  precision of TIMS, it has been successfully used for geochronology of detrital zircon grains in numerous studies (Scott and Gauthier, 1996; Machado and Gauthier, 1996; Scott, 1997) and the precision and accuracy are adequate for detrital analysis. LAM-ICP-MS has the advantage of being a relatively quick and cost effective analytical procedure capable of producing large amounts of data, required for detrital analysis, within a short period of time.

Ages were determined using  $^{207}\text{Pb}$ – $^{206}\text{Pb}$  ratios (Table 1) as U–Pb dates require multiple analyses for statistical validity, which is not feasible on a single detrital grain. The U–Pb and Pb–Pb methods of geochronology are based on the decay of  $^{235}\text{U}$ – $^{207}\text{Pb}$  and  $^{238}\text{U}$ – $^{206}\text{Pb}$ . Ideally, zircon grains will remain as a closed system thereby retaining all parent and daughter isotopes so that age calculations from each geochronometer are concordant. In reality, temperature and fluid interaction often open the grain to diffusion, resetting these values. This can be corrected in igneous-derived zircon separates, assuming there has been a single episode of lead loss and the zircons from a sample were generated from a single event. This is not possible in detrital populations because detrital grains within a single sample cannot be genetically related and therefore cannot be statistically grouped and plotted on a U–Pb concordia diagram. However, in the given data set (Table 1), when  $^{235}\text{U}$ – $^{207}\text{Pb}$  and  $^{238}\text{U}$ – $^{206}\text{Pb}$  ratios are compared, approximately 20 measurements (bold type, Table 1) fall on concordia indicating their isotopic systems are unperturbed. Most (>90%) of the measurements do not fall on concordia and cannot be represented by discords and, therefore, the  $^{207}\text{Pb}$ – $^{206}\text{Pb}$  ratios are used and the ages are considered minima.

U and Th contents in zircons reflect the source rocks in which they crystallized. Zircons in kimberlites contain the lowest U/Zr, at 0.00001, and although basaltic and ultramafic rocks generally do not contain zircon, when present, it also has low U/Zr ratios (Speer, 1980). Granites, nepheline syenite, and granitic

gneiss contain U-enriched zircons, with granitoid zircons typically having U/Zr ratios higher than 0.0006, equivalent to concentrations of >300 ppm of uranium. However, the highest typical U/Zr values from zircons are found in pegmatites in igneous intrusions associated with uranium- or thorium-bearing minerals, with U/Zr ratios as high as 0.1, or 50,000 ppm U (Speer, 1980).

The uranium content of the Thelon zircons is estimated using the U/Zr ratio (Table 1). The uranium contents correspond to low (0–0.002 U/Zr) moderate (0.003–0.006 U/Zr) and high (>0.006 U/Zr) contents, where high values roughly correspond to the uranium content of zircons from the Brownell pluton which have 1500–2300 ppm U (McNicoll et al., 1992). Analytical error is 10% based on repeat analysis within single grains.

#### 4.2. Stable isotope mass spectrometry

Analyzed quartz grains represent a fraction of one percent of the approximately 30–40 g sub-samples processed from the sampled intervals. Quartz grains were handpicked from ultrasonically cleaned sand-sized fractions. Most samples were free of overgrowths, however, highly silicified samples were treated in HF for 1 h prior to isotopic analysis. In some instances both clear and milky quartz grains were observed under the binocular microscope and were therefore separated into distinct populations for multiple analyses. In these samples, multiple analyses indicate a slight variation in  $\delta^{18}\text{O}$  from a single horizon (Table 2). However, the milky quartz populations fell within 1‰ of the clear quartz and were neither consistently higher or lower indicating there is no correlation between the clarity of quartz grains and their source.

Savin and Epstein (1970) first proposed the possibility of using oxygen isotopes of detrital quartz grains as an indication of provenance. They determined that igneous-derived quartz in beach sands normally have low  $\delta^{18}\text{O}$  values of ca. 8–10‰ whereas sands from regionally metamorphosed terranes were  $\delta^{18}\text{O}$  enriched with values of ca. 10–16‰. Since their study, oxygen isotopes have been used successfully to evaluate the nature of source terranes in other environments such as Paleoproterozoic quartz-pebble conglomerates (e.g. Vennemann et al., 1992).

Table 2  
 $\delta^{18}\text{O}$  values (in ‰) for detrital quartz grains of the eastern Thelon Basin

Drill hole	Depth (m)	Grain size (mm)	$\delta^{18}\text{O}$ mean (‰)	Error	$\delta^{18}\text{O}$ range (‰)	<i>n</i>
Upper sequence						
DPR-6	96	1.0	11.7	±0.2	—	1
	124	1.5	10.1	±0.2	—	1
	170	0.8	11.9	±0.2	—	1
	193	1.0	8.8	±0.2	7.7–9.9	2
	244	1.0	10.7	±0.2	—	1
	270	0.8	9.9	±0.2	9.7–10.1	2
	309	0.5	10.4	±0.2	—	1
	318	1.0	10.0	±0.2	—	1
	322	1.0	11.1	±0.2	—	1
	DPR-9	77	0.9	10.2	±0.2	—
H80-10-1	135		10.2	±0.2	10.1–10.2	2
	130		9.1	±0.2	7.8–10.4	2
	170		11.4	±0.2	10.2–13.2	3
H80-6-1	50		10.8	±0.2	9.4–12.2	2
	160		10.5	±0.2	9.9–11.2	3
Middle sequence						
DPR-6	394	0.4	12.0	± 0.2	—	1
	487	0.5	10.9	±0.2	—	1
	507	0.3	10.7	±0.2	—	1
	508	0.5	9.8	±0.2	—	1
	521	1.5	11.0	±0.2	9.4–12.5	5
	522	0.8	11.4	±0.2	10.8–12.0	2
	563	0.3	10.8	±0.2	9.9–11.6	2
	600	1.0	10.2	±0.2	9.4–10.9	2
	606	0.8	11.0	±0.2	—	1
	DPR-8	15	0.8	11.9	±0.2	—
21		1.5	12.7	±0.2	—	1
DPR-12	104	0.9	10.6	±0.2	—	1
	127	0.5	11.5	±0.2	—	1
H80-2-2	26	0.5	11.0	±0.2	—	1
	135	0.5	11.4	±0.2	—	1
H80-4-1	150		11.4	±0.2	10.6–12.9	3
	210		10.4	±0.2	10.1–10.7	2
	250		9.7	±0.2	9.6–9.7	2
Lower sequence						
DPR-6	614	0.5	9.8	±0.2	—	1
	616	0.3	10.6	±0.2	10.2–10.9	2
	626	0.5	13.9	±0.2	—	1
DPR-9	376	0.4	11.5	±0.2	—	1
	451	0.3	13.0	±0.2	—	1
DPR-12	236	0.7	10.4	±0.2	—	1

Each analysis represents the average value of about 1% of the typical coarse to medium fraction of detrital quartz for the sampled interval.

Oxygen isotope compositions were analyzed by dual inlet mass spectrometry and determined using the  $\text{BrF}_5$  technique of Clayton and Mayeda (1963). Isotopic analyses are reported using the ‰ notation relative to V-SMOW. Reproducibility of  $\delta^{18}\text{O}$  was determined using NIST-28 ( $\delta^{18}\text{O} = 9.60\text{‰}$ ) and is  $\pm 0.2\text{‰}$ .

## 5. Results

### 5.1. Lower sequence

The lower sequence is represented in drill holes DPR 6, DPR 9 and DPR 12, the latter of which

intersects the sub-Thelon Formation unconformity at 240 m (Fig. 3). Zircons were extracted from hematite-leached, moderately sorted, medium to very coarse sandstones from the base of fluvial cycles. These are typically 100–450  $\mu\text{m}$ , subrounded to rounded, white, elongated grains (Table 1). In the well-sorted nearshore facies, zircons were sampled from gray-green, medium-grained sandstone. These zircons are mixed in size, morphology, and color (Table 1).

Zircon ages from the lower sequence range from 2849 to 1846 Ma (Table 1). The majority cluster between 2700 and 2500 Ma with a peak at ca. 2540 Ma (Fig. 5). The Neoproterozoic and early Paleoproterozoic populations, which include more than 90% of the zircons found in the lower sequence, have moderate to low U contents (Fig. 6). On the basis of their U/Zr ratios (Fig. 6), the middle Paleoproterozoic zircons are bimodally distributed, being U-rich ( $>0.006$  U/Zr) or U-poor ( $<0.003$  U/Zr).

Quartz grains of the nearshore facies are typically polycrystalline, well-rounded and often exhibit well-developed quartz overgrowths. Detrital quartz from the fluvial sequences are polycrystalline with a relatively high percentage of equant-fine-subgrained quartz. Fluid inclusions in quartz from the lower sequence are found both as solitary, two phase aqueous–vapor inclusions up to 25  $\mu\text{m}$  and as very small aqueous inclusions that form numerous planes cross-cutting the grains indicating they are secondary in nature. Mineral inclusions in quartz throughout the sequence include zircon, apatite and tourmaline.

Quartz grains in the lower sequence have  $\delta^{18}\text{O}$  values from 9.8 to 13.9‰ (Fig. 7) suggesting dominance of a metasedimentary source with relatively low input from igneous rocks, although some zircons from this sequence have high uranium which is typical of an igneous source (Speer, 1980). However, middle Paleoproterozoic zircons, which contain the highest uranium contents, account for very few zircons within the total population.

## 5.2. Middle sequence

The middle sequence is represented in drill holes DPR-6, DPR 8 and DPR-12 (Fig. 3). Zircons occur exclusively in 5–10 cm, gray-green or mottled mudstone horizons within fluvial facies rocks. The zircons recovered are typically rounded to sub rounded

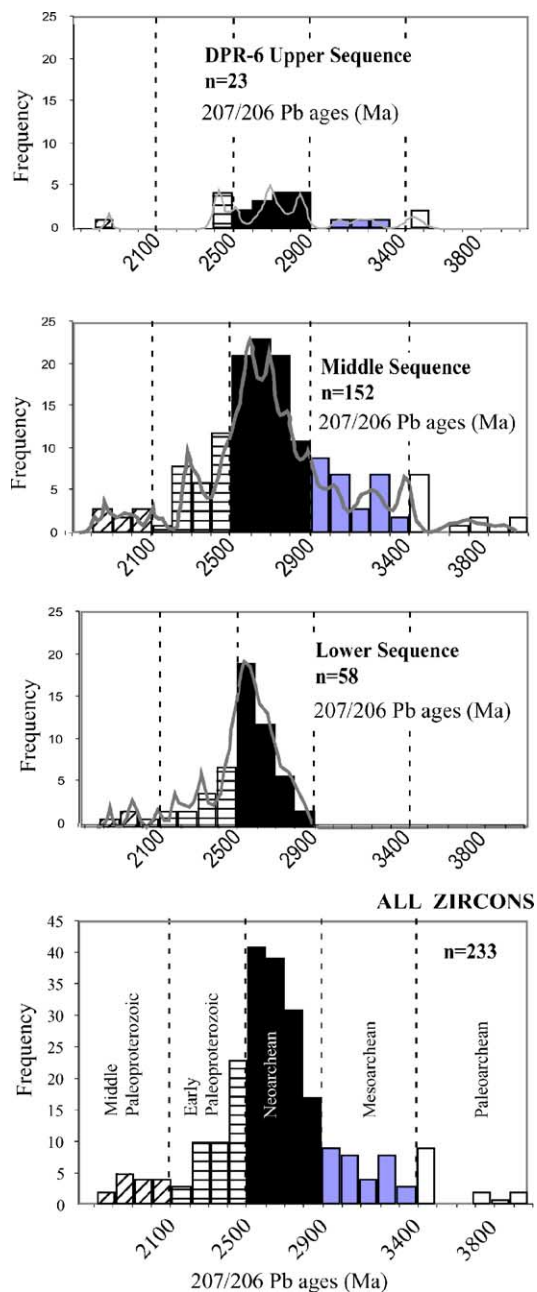


Fig. 5.  $^{207}\text{Pb}$ – $^{206}\text{Pb}$  ages of detrital zircons from the lower, middle and upper sequences of the eastern Thelon Basin shown as histogram.  $^{207}\text{Pb}$ – $^{206}\text{Pb}$  ages of zircon populations are based on several analysis per grain. The bottom histogram indicates the age distribution of all zircons used in this study. Curves represent the cumulative probability of ages based on the range of multiple analysis of single grains. Data are from Table 1.

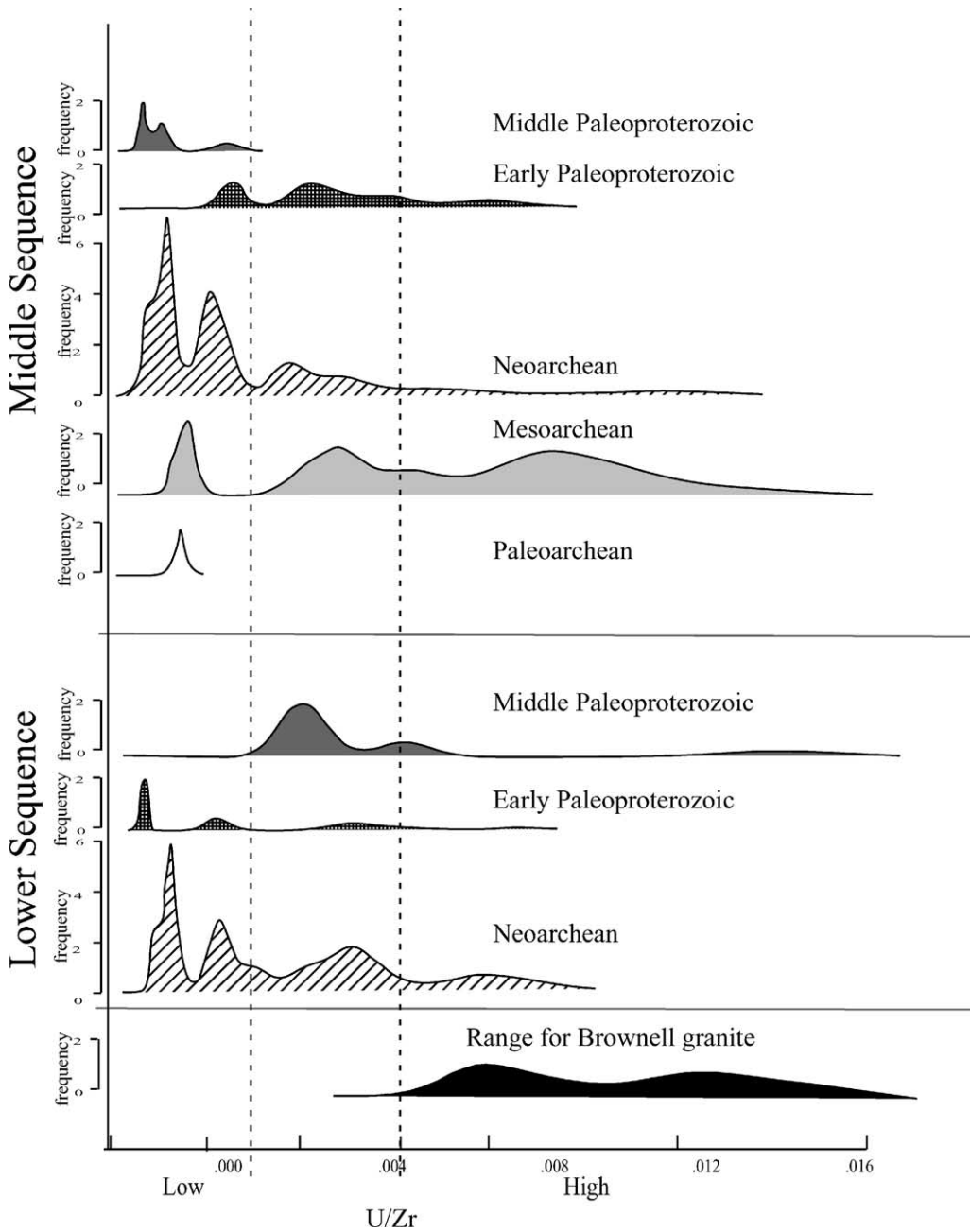


Fig. 6. U/Zr ratios of zircons from the middle and lower sequences analyzed for geochronology of the eastern Thelon Basin. The lower box indicates the range of U/Zr for the Brownell zircons which have uranium concentrations between 1500 and 2300 ppm (McNicol et al., 1992).

and up to 500  $\mu\text{m}$  long, not zoned, and some have rounded overgrowths indicating geochemical alteration prior to their deposition in the eastern Thelon Basin.

In the northern part of the eastern Thelon Basin, zircons were recovered from nearshore facies in an interval of red well-sorted medium-grained sandstone with clay laminations and in bleached coarse-grained

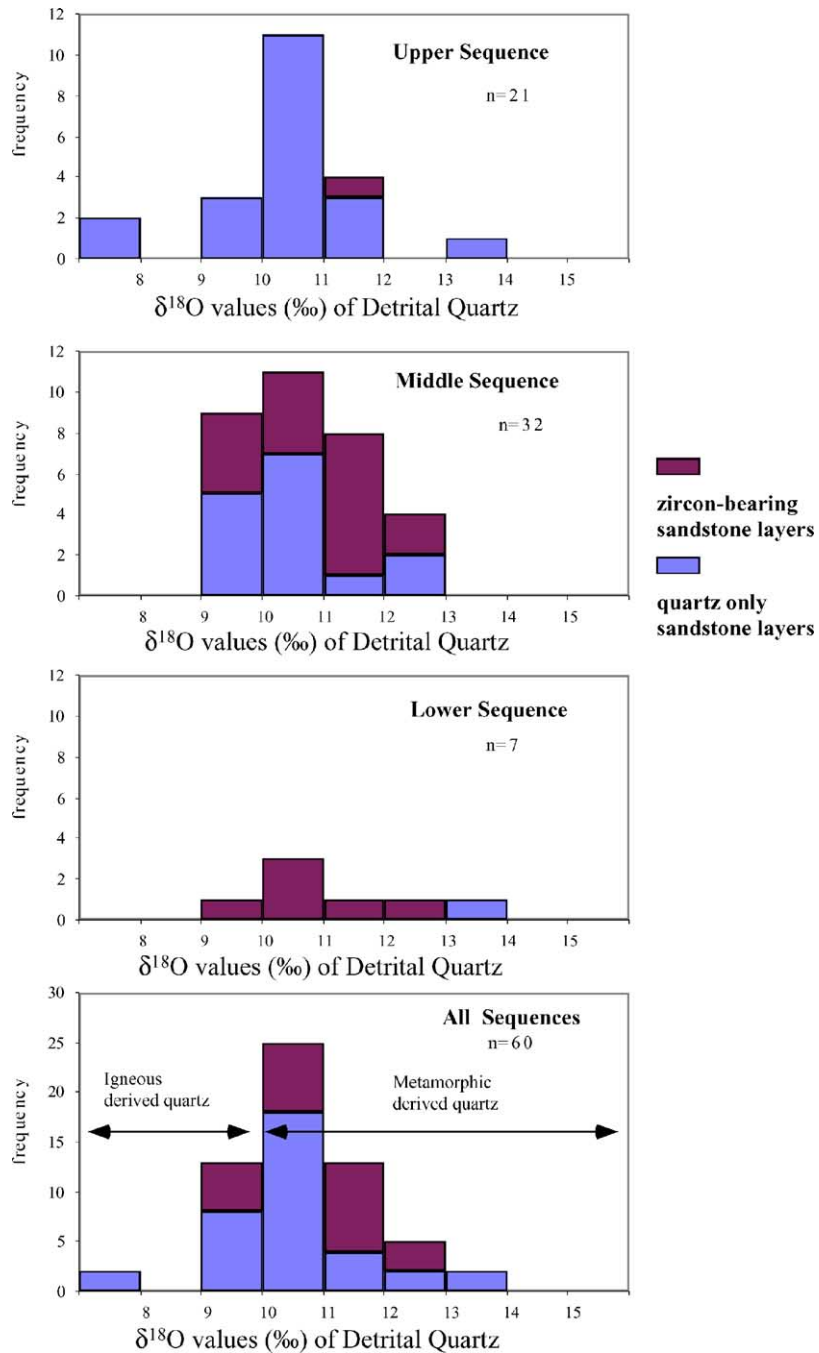


Fig. 7. Histograms of  $\delta^{18}\text{O}$  values of detrital quartz from drill holes DPR-6, DPR-8, DPR-9, and DPR-12; and H80-4-1, H80-6-1, and H80-10-1 divided into lower, middle and upper sequences. The lower histogram shows the distribution from all quartz analyses undivided by sequence. The dark grey boxes indicate  $\delta^{18}\text{O}$  values of detrital quartz grains picked from zircon-bearing horizons. Light grey boxes indicate analysis from layers bearing quartz only. Data from Table 2.

fluvial sandstones with heavy mineral bands. Most zircons are less than 200  $\mu\text{m}$ , rounded and typically brown. Quartz grains from these horizons have some partially preserved overgrowths but commonly exhibit cusped edges indicating dissolution.

Zircon ages range from 3938 to 1778 Ma, including Paleoproterozoic (>3400 Ma) zircons, the oldest population from the eastern Thelon Basin (Fig. 5). The predominant zircon population reflects a Neoproterozoic source, which peaks at ca. 2700 and 2850 Ma, and contains concordant zircons at ca. 2600, 2700, and 2850 Ma (Table 1). Relatively few zircons have middle Paleoproterozoic ages, but several zircons cluster in the early Paleoproterozoic between 2500 and 2200 Ma with a peak at ca. 2440 Ma (Fig. 5). From this latter population, approximately 10% of the zircons produced similar  $^{207}\text{Pb}$ – $^{206}\text{Pb}$  and U–Pb ages, most commonly between 2508 and 2431 Ma (Table 1), indicating the isotopic systems have not been disturbed.

There is a strong contribution from Mesoproterozoic zircons (Fig. 5) between 3400 and 2900 Ma, and these include concordant zircon ages near 3243 Ma. Although the U contents are variable, they are nevertheless the most U-rich zircons in the eastern Thelon Basin (Fig. 6) with U/Zr ratios in the range of comparable zircons from the Brownell granite. Paleoproterozoic, 300  $\mu\text{m}$ , subrounded, brown zircons range in age from 3938 to 3642 Ma (Table 1), and are found exclusively in the central part of the eastern Thelon Basin (Fig. 2).

Drill core DPR-8 intersects the sub-Thelon unconformity at a depth of 95 m. Zircons occur in heavy mineral bands in red, ripple-laminated, well-sorted, medium-grained sandstones of the nearshore facies in the upper 25 m of section. These horizons have previously been interpreted as lower sequence (Hiatt et al., 2003) because they are immediately above the basal unconformity (Fig. 3). Zircons from these intervals are abundant, rounded and range from clear to white, pale brown, orange and brown. The uppermost interval contains Mesoproterozoic zircons. Quartz grains are rounded with thick quartz overgrowths (Fig. 4a) and relatively few fluid inclusions. Approximately 5% of all polycrystalline grains contain stretched and sub-grained internal texture consistent with a metamorphic origin.

The  $\delta^{18}\text{O}$  values of quartz from the middle sequence are similar to quartz from the lower sequence (Fig. 7)

ranging from 9.4 to 12.7‰. Fluid inclusions in quartz, which are typically two-phase aqueous–vapor, or more rarely, three-phase aqueous–vapor–salt, are less abundant than in the lower and upper sequences.

### 5.3. Upper sequence

Strata from the upper sequence are found in drill holes DPR 6 and 9 (Fig. 3). Zircons were recovered from both, but those from DPR-9 were altered and contained significant common lead. Heavy mineral concentrations occur in coarse-grained purple sandstone, which yielded a mix of brown, white and clear zircons. The zircons are subrounded and small, never exceeding 200  $\mu\text{m}$ . Recovery is poor compared to other sequences probably due to intense late (ca. 1000 Ma) fluid alteration (Renac et al., 2002). The few zircons that could be extracted from the upper sequence indicate mainly Neoproterozoic to early Paleoproterozoic sources. Thirteen zircons were successfully analyzed with ages ranging from 3457 to 1885 Ma (Fig. 5). Three zircons yield ages between 2500 and 2440 Ma, indicating a proportionally greater contribution from early Paleoproterozoic sources compared to lower and middle sequences (Fig. 5). A single zircon (6-170 H) yielded concordant ages of 2847 and 2703 Ma suggesting the former was an inherited core.

Quartz grains are often corroded and overgrowths are rarely preserved. Most grains are polycrystalline and exhibit undulatory extinction. Monocrystalline grains contain abundant fluid inclusions that are less than 5  $\mu\text{m}$  and crosscut the grain in several directions oblique to the grain boundary. The  $\delta^{18}\text{O}$  values are 7.7–13.2‰ with a mean of 10.5‰ (Fig. 7). They show the greatest range and extend to lowest values (<8‰), consistent with a greater contribution from igneous sources.

## 6. Discussion

### 6.1. Pb–Pb dates from zircons

Detrital zircons can be divided into five distinct populations that represent minimum source ages based on  $^{207}\text{Pb}$ – $^{206}\text{Pb}$  ages. Most have Neoproterozoic ages (Fig. 5) consistent with the age of metasedimentary and gneissic basement rocks that surround the basin (Fig. 2) and

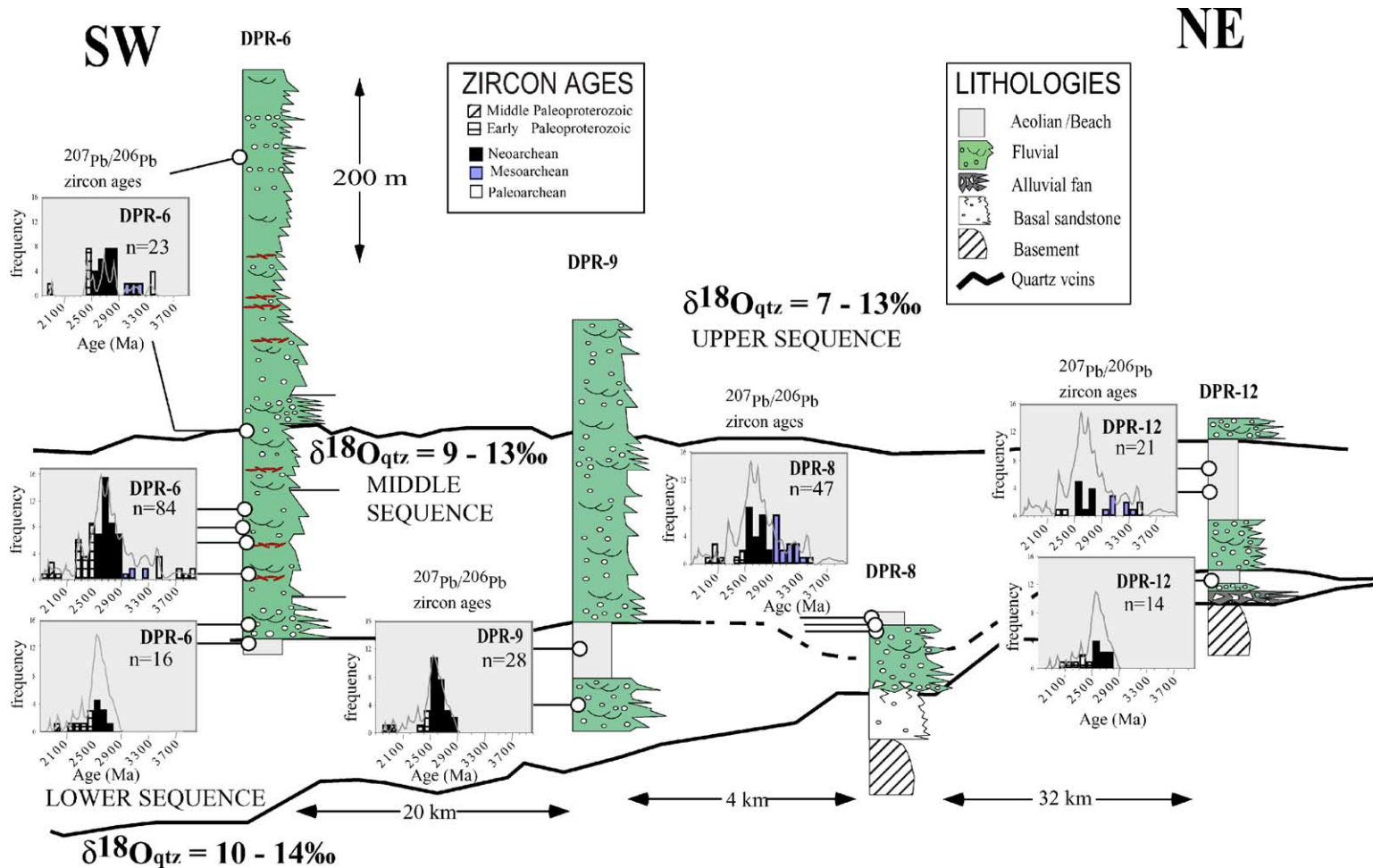


Fig. 8. Stratigraphic sections sampled for this study with the age populations (Pb–Pb ages) from each sampled interval shown in boxes to the left of the columns. Ranges of  $\delta^{18}\text{O}$  values from detrital quartz are indicated in bold typeface.

that are ubiquitous in the western Churchill (Fig. 1). Most ages probably reflect metamorphism and/or sedimentary recycling in supracrustals. However discrete older and younger populations, unique to different sequences must be explained.

Neoproterozoic zircons range from 2900 to 2500 Ma and are found consistently throughout the eastern Thelon Basin (Fig. 8). U/Zr ratios are typically U-poor in both the middle and lower sequence. Peak ages are ca. 2540 Ma in the lower sequence, at ca. 2850, 2700, and 2600 Ma in the middle sequence and ca. 2850 and 2700 Ma in the upper sequence. The older ages are easily explained by Archean gneiss and metasediments surrounding the eastern Thelon Basin. The ca. 2500 Ma ages correspond either to metamorphism and felsic magmatism (Davis et al., 2000) in the Hearne domain south of the Baker Lake Basin (Fig. 1) or, more likely, granite intrusions and orthogneisses reported in the Woodburn Lake Group (Davis and Zaleski, 1998).

Early Paleoproterozoic zircons cluster between 2500 and 2250 Ma (Fig. 5) and occur in all three sequences (Fig. 8). Older 2500–2400 Ma zircons have the highest relative abundance in the upper sequence (Fig. 5). The upper sequence contains igneous and metamorphic quartz and zircons with peak ages at 2450, 2700, and 2850 Ma. The  $^{207}\text{Pb}$ – $^{206}\text{Pb}$  ages in this paper are considered minima, and all but two analysis from the upper sequence are discordant. One concordant age at  $2627 \pm 17$  and the range of discordant ages between 2440 and 2534 (Table 1) are interpreted to represent disturbed isotopic systems in the zircons from 2.58 to 2.6 Ga granites. This is supported by  $^{207}\text{Pb}$ – $^{206}\text{Pb}$  ages of 2606–2432 Ma reported by LeCheminant and Roddick (1991) for zircons extracted from plutons surrounding the study area.

Few zircons with ages between 2250 and 2150 Ma are found in the eastern Thelon Basin. Middle Paleoproterozoic zircons range from 2098 to 1778 Ma and occur in all three sequences (Fig. 5). These ages comprise only 4–6% of the analysis in any of the sequences. The lack of 1760–1830 Ma ages reflects the paucity of zircons in the Wharton and Baker Lake Groups, a thick succession of felsic volcanics and sediments interpreted as 1.84–1.79 Ga (Rainbird and Hadlari, 2000 and references therein), that underlie the Thelon Formation to the south (Fig. 2). Middle Paleoproterozoic zircons are generally zoned and probably indicate a small contribution from detrital grains

within the Baker Lake Basin and/or coeval granitoid plutonism (Peterson et al., 2000) that surrounds the basin. Local paleocurrents indicate drainage from the south (Fig. 2). Wharton and Baker Lake Group derived zircons are probably limited to the lower sequence near the southern margin. The Thelon Formation probably extended much further south based on the >400 m thickness of the Thelon Formation near the present southern limits of the basin.

The oldest zircon population is Paleoproterozoic and occurs in the middle and upper sequences with a cluster of ages between 3457 and 3400 Ma and a few ages older than 3600 Ma (Fig. 8). Archean detrital zircons with ages of 3000–2810 Ma occur in polymictic conglomerate and orthoquartzite in the Woodburn Lake Group (Davis and Zaleski, 1998), suggesting a proximal Mesoproterozoic source. Recent data indicates detrital zircons in the orthoquartzite may be as old as 3500 Ma (Zaleski et al., 2000).

Ages greater than 3500 Ma are more difficult to attribute to nearby sources. Paleoproterozoic outcrops of this age are uncommon in the Canadian Shield, although detrital or inherited zircons of these ages have been documented in three areas (Fig. 9). To the east of the Thelon Basin, in the hinterland of the Torngat Orogen (Fig. 1), rounded inclusions within igneous zircons of the Uivak gneiss record ages of 3860–3730 Ma (Schiotte et al., 1992). To the south of the Trans-Hudson Orogenic belt in the Assean Lake complex of the Western Superior Province (Fig. 1), detrital zircons in metagreywacke record ages up to 3900 Ma (Bohm et al., 2001). To the west, the Slave Province contains extensive Archean granite–greenstone terranes. Detrital zircons extracted from quartzite in the Central Slave Cover Group reveal ages from 3950 to 2600 Ma, with peak accumulations at ca. 3400, 3150, 2900, and 2825 Ma, and minor populations at 3950–3600 Ma (Bleeker et al., 2000). Ages older than 3900 Ma are recorded in the Acasta gneiss (Stern and Bleeker, 1998). These exposures all occur far from the present position of the eastern Thelon Basin.

If Paleoproterozoic zircons of the middle sequence were to have come directly from the Western Superior, Nain, or Slave provinces, they would have to have been transported across major orogenic belts, the Trans-Hudson, Torngat, and Thelon–Talston, respectively, which likely constituted drainage divides.

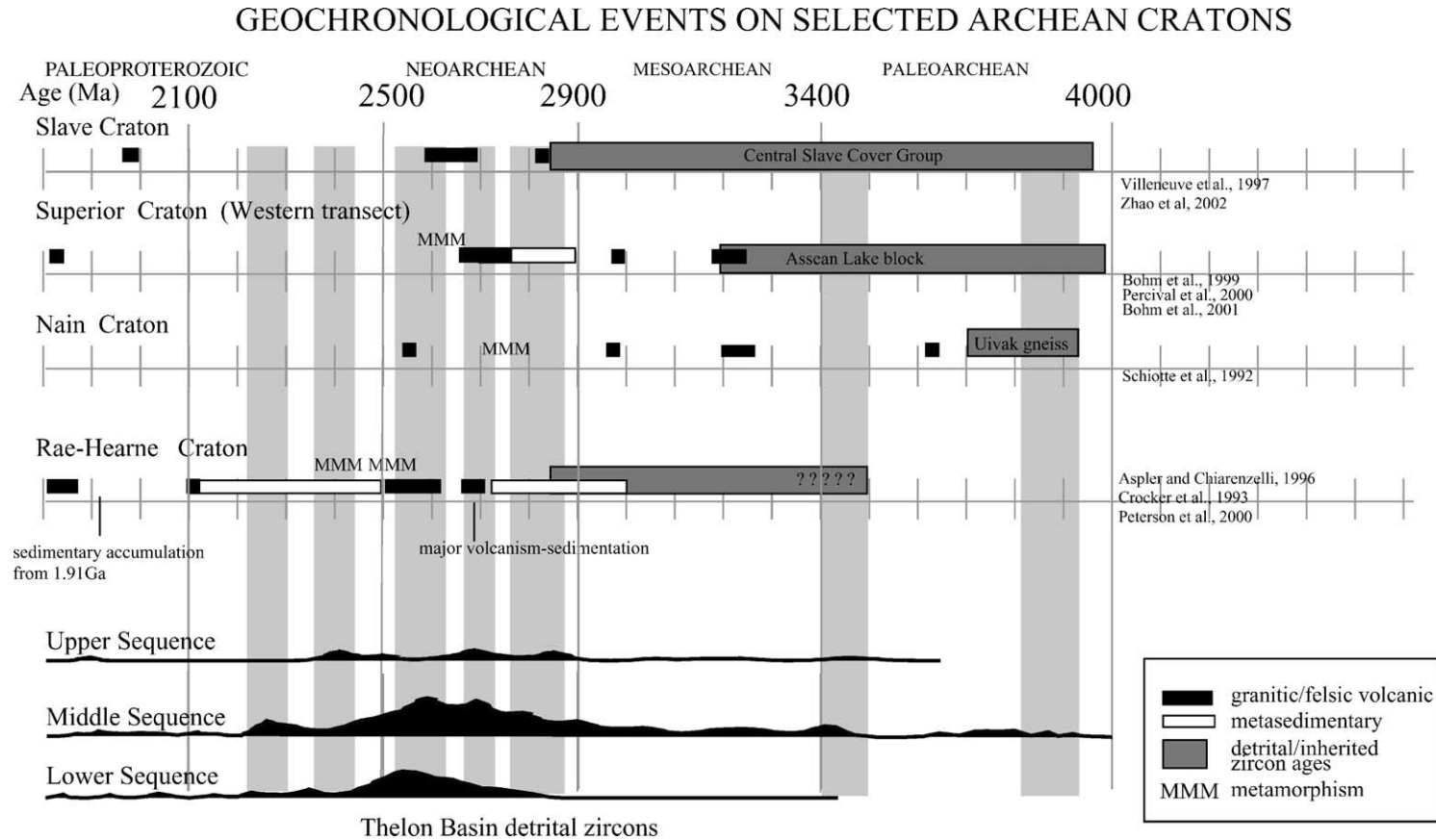


Fig. 9. Geochronological histories of selected cratons indicating periods of magmatism, age of supracrustal accumulation and age of the oldest detrital zircons found to date. Also shown are the cumulative probability ages from the sequences in the eastern Thelon Basin (Crocker et al., 1993; Percival et al., 2000; Villeneuve et al., 1997).

Furthermore, the Trans-Hudson Orogenic Belt includes the extensive 1850 Ma Wathaman Batholith (Fig. 1) which could also have been a barrier to sediment transport. Less than 2% of all zircons analyzed from the eastern Thelon Basin are of this age, which suggests that if the Superior was the source of the oldest detrital zircons, they were not transported across the Trans-Hudson. More likely, they could have been deposited into an older basin and subsequently reworked to arrive and carried into the Thelon Basin.

Paleocurrents suggest the primary drainage direction was from the east to the west (Fig. 1) during deposition of the Thelon Basin (Donaldson, 1965). However, if the zircons have been recycled it would be difficult to ascertain provenance solely by age and paleocurrents. Pan-continental drainage systems have been documented (Rainbird et al., 1997; Aspler et al., 2001) over much of the Canadian Shield. During deposition of the upper part of the Hurwitz Group, and prior to deposition of the Thelon Formation, a pan-continental fluvial system drained east delivering 2.5–1.9 Ga zircons to the Hurwitz Basin south of the Thelon Basin, and possibly contributed detritus to the age-equivalent Amer Group northeast of the Thelon Basin (Aspler et al., 2001). A similar system could also have delivered older Paleoproterozoic zircons into the western Churchill Province.

The presence of Paleoproterozoic zircons in the middle sequence leads us to suggest that the oldest source material was most likely now on the order of 1000–2000 km away. However, given that there is a strong indication some zircons are recycled, coupled with the uncertainty of paleo-tectonic reconstructions for this time (e.g. Zhao et al., 2002; Karlstrom et al., 1999; Idnurm and Giddings, 1995; Moores, 1991), we can not conclusively determine the source. Because of limited exposure of bedrock east of the Thelon Basin, we cannot rule out the possibility that >3500 Ma sources may yet be discovered in the eastern Rae domain.

In hole DPR-8 Mesoarchean zircons are present approximately 80 m above the basal unconformity (Fig. 8). Zircons of this age do not occur elsewhere in lower sequence strata but zircons of similar age and U/Zr content (Table 1) are found in middle sequence strata suggesting these strata were derived from the same region as the middle sequence (Fig. 8). Detrital mineral assemblages are consistent with both the lower and middle sequences and therefore do not

conclusively determine the stratigraphic level of the strata. There are two possible explanations for the presence of Mesoarchean zircons in this stratigraphic interval, which suggest that this interval is part of the middle sequence. This area may have been a paleotopographic high during deposition of the lower sequence, or more plausibly, a middle sequence channel cut down through the nearshore facies of the lower sequence (Fig. 3), a sedimentary process in keeping with braided stream systems (Miall and Arush, 2001).

Mesoarchean (2900–3400 Ma) and Paleoproterozoic zircons of the middle sequence contain high U/Zr ratios (Fig. 6) corresponding to greater than 1500 ppm uranium. This suggests a granitic source and probably one that contained anomalously high values of uranium.

## 6.2. Oxygen isotopes from detrital quartz

Oxygen isotopic compositions from detrital quartz range from 7.7 to 13.9‰ (Table 2). The high values for each sequence are similar and the range in isotopic compositions from the lower (9.8–13.9‰), middle (9.4–12.9‰), and upper (7.7–13.2‰), sequences are close (Fig. 7). However, isotopically light (<9‰) grains only occur in the upper sequence (Fig. 7).

The lower sequence contains quartz grains that are dominantly polycrystalline, and finely subgrained quartz grains are abundant. Lithic clasts include reworked sandstone, siltstone, banded iron formation and quartzite. Zircon and apatite are common both as detrital grains and as inclusions in the detrital quartz. The  $\delta^{18}\text{O}$  values of the detrital quartz in the lower sequence of the eastern Thelon Basin indicate a metamorphic origin and are consistent with metasedimentary rocks, such as those to the east and northeast. Numerous two-phase aqueous–vapor and small, aqueous, secondary inclusions are also consistent with metasedimentary sources and vein quartz, respectively.

The middle sequence contains quartz that is typically polycrystalline and often contains abundant biotite, muscovite, tourmaline and zircon inclusions, rare pyrite inclusions and abundant high-salinity fluid inclusions. Lithic clasts, such as banded iron formation and sandstone, are present in minor amounts and are typically altered. The  $\delta^{18}\text{O}$  values of quartz, 9.4–12.9‰, suggest a predominant contribution from

metamorphic sources, but inclusions associated with igneous rocks possibly indicate an increase in the contribution from granitic sources. High-salinity fluid inclusions are consistent with a granitic-related source.

To the south, the eastern Thelon Basin is surrounded by Archean gneisses punctuated by Paleoproterozoic (ca. 1.85–1.75 Ga) monzonite to granite intrusions (Peterson et al., 2000) and the Baker Lake Basin comprising ultrapotassic volcanic rocks, sandstone and conglomerate. Quartz grains with pyrite inclusions may have been derived from large stockworks within the volcanics described by Turner et al. (2001) in the Mallory Lake area approximately 40 km to the south. Some contribution from the south is implied by the presence of reworked sandstone clasts typical of the Baker Lake basin.

Quartz from the upper sequence is both polycrystalline and monocrystalline with abundant apatite and zircon inclusions. Lithic clasts are rare. The  $\delta^{18}\text{O}$  values of quartz range from 7.7 to 13.2‰. The shift toward lower values, relative to the other sequences, without an accompanying decrease in the high end values, most likely reflects an increase in the proportion of isotopically light material. This shift indicates an influx of granitic material late in the depositional history or preferential preservation of igneous-derived quartz reworked from the lower and middle sequences.

### 6.3. Implications for Basin Evolution

The lower sequence contains zircons derived from Neoproterozoic and early Paleoproterozoic terranes. The  $\delta^{18}\text{O}$  values of quartz suggest a dominantly metamorphic source (Fig. 10). Detrital apatite is preserved indicating limited alteration during transport of material and therefore a proximal source. Because the eastern Thelon Basin is surrounded to the south, north, and east by Neoproterozoic metasedimentary sequences, early Paleoproterozoic supracrustal rocks, such as the Amer Group, and minor granitic intrusions, it is difficult to more accurately locate the source of this detritus other than to conclude it was proximal to the basin. The lower sequence contains a variety of clasts also consistent with mixed local sources.

The middle sequence, based on  $\delta^{18}\text{O}$  values, is derived from a dominantly metamorphic source (Fig. 10). Zircons from early Paleoproterozoic (>3400 Ma) to middle Paleoproterozoic (1750–2100 Ma) terranes

contribute to this sequence and the presence of banded iron formation clasts suggests derivation from southern exposures in the Hearne domain or possibly from the east in the Woodburn Lake Group. There is, however, no known proximal source area for the oldest zircons, which are >3700 Ma (Fig. 5). A potential source area is the Labrador segment of the Nain province to the east, containing the 3860–3730 Ma Uivak gneiss (Fig. 1). Other possible source terranes are the Superior province with 3900–3700 Ma detrital zircons in metasediments of the Assean Lake crustal complex (Bohm and Heaman, 1999; Bohm et al., 2001), or the metasedimentary quartzites of the Slave Province (Bleeker et al., 2000) (Fig. 9). The zircons may have been reworked from material deposited to the east of the basin prior to the 2.1–1.8 amalgamation of the Canadian Shield.

The upper sequence, sampled from DPR-6 and 9, has a similar zircon population as the middle sequence (Fig. 5), with ages from the middle Paleoproterozoic (2100–1750 Ma) to Paleoproterozoic (>3400 Ma). The scarcity of zircons in the upper sequence may be due to their poor preservation. The  $\delta^{18}\text{O}$  values of quartz are similar in all sequences but extend to lower values in the upper sequence. The upper part of the range reflects similar sources of sediment as for the lower and middle sequences (Fig. 10). This sediment could have been derived by local reworking of the lower two sequences. The lower  $\delta^{18}\text{O}$  values (Fig. 7), however, require a greater contribution of igneous rocks, such as from the nearby granite plutons that surround the Amer Group (LeCheminant and Roddick, 1991).

The analysis of detrital material indicates the nature and distance of the source areas and how they have changed through time. This in turn elucidates the paleogeographic and tectonic evolution of the basin. Integration of lithostratigraphic data, detrital zircon ages, U/Zr ratios, and  $\delta^{18}\text{O}$  values of detrital quartz indicate that early sources for the detritus that fed the basin, now represented in the lower sequence, were nearby and tectonically controlled. In contrast, older material within the fluvial-dominated middle sequence and predominant west-directed paleocurrents suggests deposition from a more distal source to the east. By the time deposition of the upper sequence commenced, detritus was again supplied from predominantly proximal sources and consisted mainly of reworked existing Thelon Formation combined

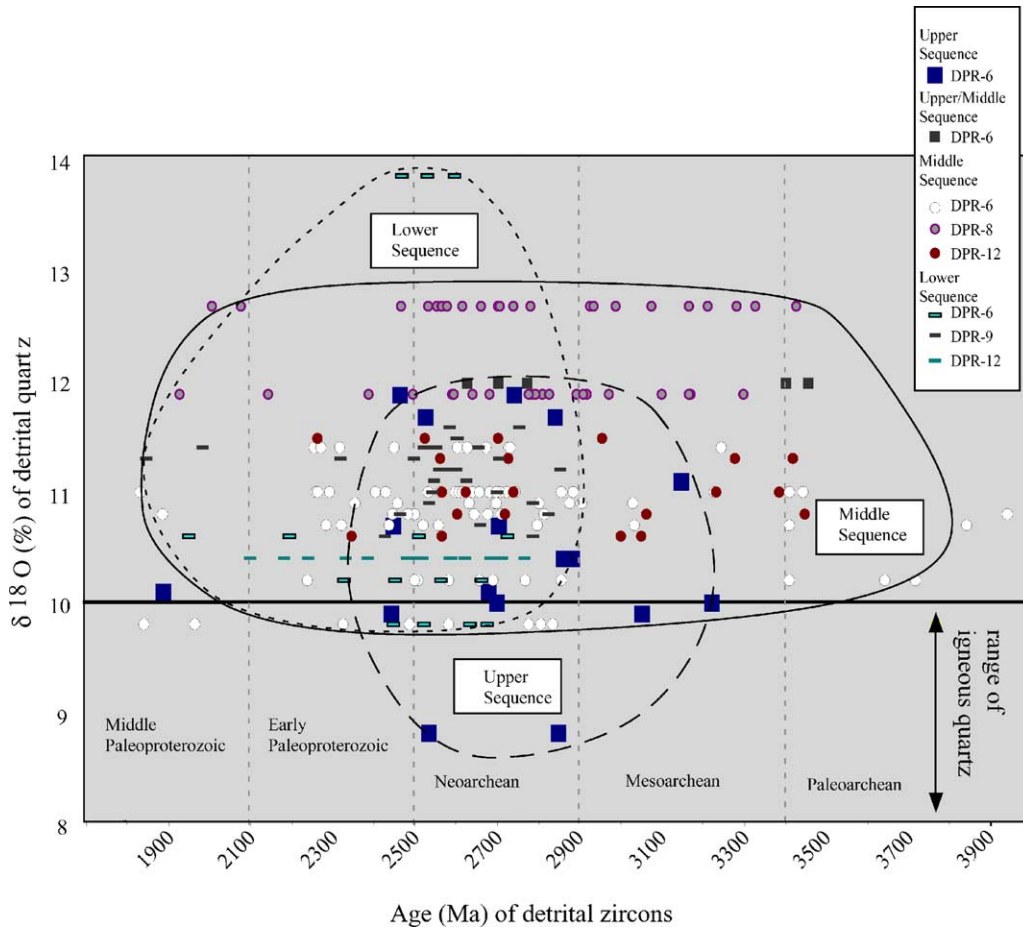


Fig. 10. Oxygen isotope composition from detrital quartz (approximately 1% of the quartz grains in a sample) plotted against the  $^{206}\text{Pb}$ – $^{207}\text{Pb}$  ages from single zircon grains from the same sample. Where several analyses are represented in the sampled horizon, a range of age values are given.

with nearby granites. The detrital assemblages from lower, middle and upper sequences therefore record a change in source from proximal to distal to proximal and suggests the basin's depositional history, initially controlled by tectonic processes, was sustained by a regional paleo-slope to the west. Reworking of lower strata and a return to proximal sources record the waning stages of the fluvial system.

## 7. Summary

Initial deposition of sediment in the Thelon Basin is constrained by the youngest zircon age of  $1778 \pm$

$16$  Ma, and the unconformable contact with  $1753 \pm 3$  Ma fluorite-bearing granite (Loveridge et al., 1987). The onset of diagenesis is constrained by  $1720 \pm 6$  Ma phosphate cement (Miller et al., 1989). This indicates the basin-infilling event spanned a period of no more than 33 Ma, during which time the drainage systems expanded and then contracted. Based on sediment composition,  $^{207}\text{Pb}$ – $^{206}\text{Pb}$  ages of detrital zircons, and oxygen isotopic compositions of detrital quartz (Fig. 10), the early detrital material in the lower sequence was derived predominantly from the proximal Neoproterozoic and Paleoproterozoic metasediments surrounding the eastern Thelon Basin. Early block-faulting of the basin probably controlled deposition.

Detrital material of the middle sequence was derived in part from similar sources (Fig. 10) but also included Paleoarchean and Mesoarchean material probably derived from the east, perhaps as far away as 1000–2000 km, and transported via drainage systems controlled by a regional paleoslope. The distinct absence of Paleo and Mesoarchean zircons from the lower sequence generally supports the stratigraphic subdivisions of the eastern Thelon Basin established by Hiatt et al. (2003) suggesting only minor modification: the reassignment of the upper portion of DPR-8 from the lower sequence to the middle sequence.

The upper sequence includes material of the same age range as the middle sequence but pristine zircons are rare and lower  $\delta^{18}\text{O}$  values (Fig. 10) indicate a greater contribution from felsic igneous sources suggesting a more proximal source and local reworking of earlier Thelon Formation strata. This return to a more local provenance coupled with the coarse-grained fluvial deposits that comprise this sequence, suggest renewed uplift at the basin margins.

## Acknowledgements

We thank the people of Cameco Corporation, most notably, Garth Dreaver, Ted O’Conner, Charles Roy, and Dave Thomas for field support and invaluable conversation. We also thank Kerry Klassen, Don Chipley and Paul Polito of Queen’s University for invaluable technical assistance and insightful comments and reviewers Lawrence Aspler and Peter Cawood for comments and suggestions that have greatly improved the manuscript. This project was funded by Cameco Corporation and through an NSERC CRD grant to K.K.

## References

- Aspler, L.B., Chiarenzelli, J.R., 1996. Stratigraphy, sedimentology and physical volcanology of the Henik Group, central Ennadai-Rankin greenstone belt, Northwest Territories, Canada: late Archean paleogeography of the Hearne Province and tectonic implications. *Precambrian Res.* 77, 59–89.
- Aspler, L.B., Chiarenzelli, J.R., Cousens, B.L., McNicoll, V.J., Davis, W.J., 2001. Paleoproterozoic intracratonic basin processes, from break-up of Kenorland to assembly of Laurentia: Hurwitz Basin, Nunavet, Canada. *Sed. Geol.* 141–142, 287–318.
- Bohm, C.O., Heaman, L.M., 1999. Archean crustal evolution of the northwestern Superior craton margin: U–Pb zircon results from the Split Lake Block. *Can. J. Earth Sci.* 36, 1973–1987.
- Bohm, C.O., Heaman, L.M., Creaser, R.A., Corkery, M.T., Stern, R.A., 2001. Two billion years of crustal evolution preserved at the NW Superior Craton margin. In: Harrup, R.M., Helmstaedt, H.H. (Eds.), *Proceedings of the Western Superior Transect Seventh Annual Workshop*. Lithoprobe Report, vol. 80, pp. 29–35.
- Bleeker, W., Ketchum, J., Tomlinsion, K., Thurston, P., Sircombe, K., Stern, R., Davis, D., 2000. Archean quartzite-banded iron formation-komatiite sequences: indicators of rifting of Mesoarchean supercratons. In: *GeoCanada 2000 Meeting*, May, 2000, Calgary, Alberta. Abstract #1189 (CD format).
- Cawood, P.A., Nemchin, A.A., 2001. Paleogeographic development of the East Laurentian margin constraints from U–Pb dating of detrital zircons in the Newfoundland Appalachians. *Geol. Soc. Am. Bull.* 113, 1234–1246.
- Clayton, R.N., Mayeda, T.K., 1963. The use of bromine pentafluoride in the extraction of oxygen from oxides and silicates for isotopic analysis. *Geochim. Cosmochim. Acta* 27, 43–52.
- Crocker, C.H., Collerson, K.D., Lewry, J.F., Bickford, M.E., 1993. Sm–Nd, U–Pb, and Rb–Sr geochronology and lithostructural relationships in the southwestern Rae Province: constraints on crustal assembly in the western Canadian Shield. *Precambrian Res.* 61, 27–50.
- Davis, W.J., Zaleski, E., 1998. Geochronological investigations of the Woodburn Lake group, western Churchill Province, Northwest Territories: preliminary results. In: *Radiogenic Age and Isotopic Studies*, Report 11. Geological Survey of Canada, Current Research 1998-F, pp. 89–97.
- Davis, W.J., Hanmer, S., Aspler, L., Sandeman, H., Tella, S., Zaleski, E., Relf, C., Ryan, J., Berman, R., MacLachlan, K., 2000. Regional differences in the Neoproterozoic crustal evolution of the Western Churchill Province: can we make sense of it? In: *GeoCanada 2000 Meeting*, May, 2000, Calgary, Alberta. Abstract #864 (CD format).
- Donaldson, J.A., 1965. The Dubawnt Group, districts of Keewatin and Mackenzie. *Geological Survey of Canada Paper* 64-20, p. 11.
- Fraser, J.A., Donaldson, J.A., Fahrig, W.F., Tremblay, L.P., 1970. Helikian basins and geosynclines of the northwestern Canadian Shield. In: Baer, A.J. (Ed.), *Basins and Geosynclines of the Canadian Shield*. Geological Survey of Canada Paper 70-40, pp. 213–238.
- Gall, Q., Peterson, T.D., Donaldson, J.A., 1992. A proposed revision of early Proterozoic stratigraphy of the Thelon and Baker Lake basins, Northwest Territories. Current research; Part C, Canadian Shield, Geological Survey of Canada Paper 92-01C, pp. 129–137.
- Heaman, L., Parrish, R., 1991. U–Pb geochronology of accessory minerals. In: Heaman, L., Ludden, J.N. (Eds.), *Applications of Radiogenic Isotope Systems to Problems in Geology Short Course Handbook*, Short Course Handbook, vol. 19, pp. 59–102.
- Hiatt, E.E., Kyser, T.K., Dalrymple, R.W., 1999. Sequence stratigraphy of the Proterozoic Thelon Formation, Nunavut Territory, Canada: accommodation space and systems tracts in

- an ancient fluvial-dominated clastic system. *Geol. Soc. Am. Abstr. Progr.* 31, 424.
- Hiatt, E.E., Kyser, T.K., Dalrymple, R.W., 2003. Relationships among sedimentology, stratigraphy and diagenesis in the Proterozoic Thelon Basin, Nunavut, Canada: implications for paleo-aquifers and sedimentary-hosted mineral deposits. *J. Geochem. Explor.* 80, 221–240.
- Hoffman, P.F., 1990. Subdivision of the Churchill Province and extent of the Trans-Hudson Orogen. In: Lewry, J.F., Stauffer, M.R. (Eds.), *The Early Proterozoic Trans-Hudson Orogen of North America*. Geological Association of Canada, Special Paper 37, pp. 15–40.
- Idnurm, M., Giddings, J.W., 1995. Paleoproterozoic-Neoproterozoic North America-Australia link; new evidence from paleomagnetism. *Geology* 23, 149–152.
- Jackson, M.J., Pianosi, J.G., Donaldson, J.A., 1984. Aeolian dunes in early Proterozoic Thelon Formation near Schultz Lake, central Keewatin. *Geological Survey of Canada Paper* 84-1B, pp. 53–63.
- Karlstrom, K.E., Harlan, S., Williams, M.L., McLelland, J., Geissman, J.W., Ahall, K.I., 1999. Refining Rodinia geologic evidence for the Australia-Western U.S. connection in the Proterozoic. *GSA Today* 9, 1–7.
- Kotzer, T.G., Kyser, T.K., 1995. Petrogenesis of the Proterozoic Athabasca Basin, northern Saskatchewan, Canada, and its relation to diagenesis, hydrothermal uranium mineralization and paleohydrogeology. *Chem. Geol.* 120, 45–89.
- Kroner, A., O'Brien, P.J., Nemchin, A.A., Pidgeon, R.T., 2000. Zircon ages for high pressure granulites from South Bohemia, Czech Republic, and their connection of Carboniferous high temperature processes. *Contrib. Mineral. Petrol.* 138, 127–142.
- Kyser, T.K., Hiatt, E.E., Renac, C., Durocher, K., Holk, G.J., Deckart, K., 2000. Diagenetic fluids in paleo- and meso-Proterozoic sedimentary basins and their implications for long protracted fluid histories. In: Kyser, K. (Ed.), *Fluids and Basin Evolution*. Mineralogical Association of Canada, Ottawa, pp. 225–262.
- LeCheminant, A. N., Roddick, J.C., 1991. U–Pb zircon evidence for widespread 2.6 Ga felsic magmatism in the central District of Keewatin, N.W.T. In: *Radiogenic Age and Isotopic Studies*. Report 4. Geological Survey of Canada Paper 90-02, pp. 91–99.
- LeCheminant, A.N., Ashton, K.E., Chiarenzelli, J., Donaldson, J.A., Best, M.A., Tella, S., Thompson, D.L., 1983. Geology of Aberdeen Lake map area, District of Keewatin. *Geological Survey of Canada Paper* 83-1A, pp. 437–448.
- LeCheminant, A.N., Jackson, M.J., Galley, A.G., Smith, S.L., Donaldson, J.A., 1984. Early Proterozoic Amer Group, Beverly Lake map area, District of Keewatin. *Geological Survey of Canada Paper* 84-1B, pp. 159–172.
- LeCheminant, A.N., Roddick, J.C., Tessier, A.C., Bethune, K.M., 1987. Geology and U–Pb ages of early Proterozoic calc-alkaline plutons northwest of Wager Bay, District of Keewatin. *Geological Survey of Canada Paper* 87-1A, pp. 773–782.
- Lewry, J.F., Stauffer, M.R., Fumerton, S., 1981. A Cordilleran type batholithic belt in the western Churchill Province in northern Saskatchewan. *Precambrian Res.* 14, 277–313.
- Loveridge, W.D., Eade, K.E., Roddick, J.C., 1987. A U–Pb age on zircon from a granite pluton, Kamilukuak Lake area, District of Keewatin, establishes a lower limit for the age of the Christopher Island Formation, Dubawnt Group. *Radiogenic age and isotopic studies: Report 1*, Geological Survey of Canada Paper 87-2, pp. 67–71.
- Lucas, S.B., Stern, R.A., Syme, E.C., Reilly, B.A., Thomas, D.J., 1996. Intraoceanic tectonics and the development of continental crust; 1.92–1.84 Ga evolution of the Flin Flon Belt, Canada. *Geol. Soc. Am. Bull.* 108, 602–629.
- Machado, N., Gauthier, G., 1996. Determination of  $^{207}\text{Pb}/^{206}\text{Pb}$  ages on zircon and monazite by laser-ablation ICPMS and application to a study of sedimentary provenance and metamorphism in southeastern Brazil. *Geochim. Cosmochim. Acta* 60, 5063–5073.
- MacLachlan, K., Hanmer, S., Davis, W.J., Berman, R., Ryan, J.J., Relf, C., Aspler, L.B., 2000. Complex protracted Proterozoic reworking of the Western Churchill Province: the craton that wouldn't grow up? In: *GeoCanada 2000 Meeting*, May, 2000, Calgary, Alberta. Abstract # 747 (CD format).
- McNicoll, V.J., Delaney, G.D., Parrish, R.R., Heaman, L.M., 1992. U–Pb determinations from the Glennie Lake Domain, Trans-Hudson Orogen, Saskatchewan, Radiogenic age and isotopic studies: Report 6, Geological Survey of Canada Paper 92-02, pp. 57–72.
- McNicoll V.J., Theriault, R.J., McDonough, M.R., 2000. Taltson basement gneissic rocks U–Pb and Nd isotopic constraints on the basement to the Paleoproterozoic Taltson magmatic zone, northeastern Alberta. In: Ross, G.M. (Ed.), *The Lithoprobe-Alberta basement transect–Le transect Lithoprobe du socle albertain*. *Can. J. Earth Sci.* 37, 1575–1596.
- Miall, A.D., Arush, M., 2001. Cryptic sequence boundaries in braided fluvial successions. *Sedimentology* 48, 971–985.
- Miller, A.R., Cumming, G.L., Krstic, D., 1989. U–Pb, Pb–Pb, and K–Ar isotopic study and petrography of uraniferous phosphate-bearing rocks in the Thelon Formation, Dubawnt Group, Northwest Territories, Canada. *Can. J. Earth Sci.* 26, 867–880.
- Molnar, P., Tapponnier, P., 1977. The collision between India and Eurasia. *Sci. Am.* 236, 30–41.
- Moores, E.M., 1991. Southwest U.S.-East Antarctic (SWEAT) connection a hypothesis. *Geology* 19, 425–428.
- Okulitch, A.V., 1999. Geological Time Scale. Geological Survey of Canada open file 3040.
- Patterson, J.G., 1986. The Amer Belt remnant of an Aphebian foreland fold and thrust belt. *Can. J. Earth Sci.* 23, 2012–2023.
- Percival, J.A., Bailes, A.H., Corkery, M.T., Dube, B., Harris, J.R., McNicoll, V., Panagapko, D., Parker, J.R., Rogers, N., Sanborn-Barrie, M., Skulski, T., Stone, D., Stott, G.M., Tomlinson, K.Y., Whalen, J.B., Young, M.D., 2000. Western Superior NATMAP; an integrated view of Archean crustal evolution. In: *Explore in Manitoba: Report of Activities*. Manitoba Industry, Trade and Mines, Geological Services, pp. 108–116.
- Peterson, T.D., van Breeman, O., Sandeman, H., Rainbird, R.H., 2000. Proterozoic (1.85–1.75 Ga) granitoid plutonism and tectonics of the Western Churchill Province. In: *GeoCanada 2000 Meeting*, May, 2000, Calgary, Alberta. Abstract #512 (CD format).

- Rainbird, R.H., Hadlari, T., 2000. Revised stratigraphy and sedimentology of the Paleoproterozoic Dubawnt Supergroup at the northern margin of Baker Lake Basin, Nunavut. Geological Survey of Canada, Current Research 2000-C8, 9 pp.
- Rainbird, R.H., McNicoll, V.J., Theriault, R.J., Heaman, L.M., Abbott, J.G., Long, D.G.F., Thorkelson, D.J., 1997. Pancontinental river system draining Grenville Orogen recorded by U–Pb and Sm–Nd geochronology of Neoproterozoic quartzarenites and mudrocks, northwestern Canada. *J. Geol.* 105, 1–17.
- Rainbird, R.H., Davis, W.J., Aspler, L.B., Chiarenzelli, J.R., Ryan, J.J., 2002. SHRIMP U–Pb detrital zircon geochronology of enigmatic Neoproterozoic–Paleoproterozoic sedimentary rocks of the central western Churchill Province, Nunavut. *Current Research: Geological Survey of Canada*, 2002-F5, p. 8.
- Ramaekers, P., 1981. Hudsonian and Helikian basins of the Athabasca region, Northern Saskatchewan. In: Campbell, F.H.A. (Ed.), *Proterozoic basins of Canada*: Geological Survey of Canada Paper 81-10, pp. 219–234.
- Renac, C., Kyser, T.K., Drever, G., O'Connor, T., 2002. Comparison of diagenetic fluids in the Proterozoic Thelon and Athabasca basins, Canada: implications for long protracted fluid histories in stable intracratonic basins. *Can. J. Earth Sci.* 39, 113–132.
- Ross, G.M., Parrish, R.R., Winston, D., 1992. Provenance and U–Pb geochronology of the Mesoproterozoic Belt Supergroup (northwestern United States) implications for age of deposition and pre-Panthalassa plate reconstructions. *Earth Planet. Sci. Lett.* 113, 57–76.
- Savin, S.M., Epstein, S., 1970. The isotopic compositions of coarse grained sedimentary rocks and minerals. *Geochim. Cosmochim. Acta* 34, 323–329.
- Schau, M., 1982. Geology of the Prince Albert Group in parts of Walker Lake and Laughland Lake map areas, District of Keewatin. *Geol. Surv. Can. Bull.* 337, 62.
- Schiotte, L., Nutman, A.P., Bridgewater, D., 1992. U–Pb ages of single zircons within the “Upernavik” metasedimentary rocks and regional implications for the tectonic evolution of the Nain Province, Labrador. *Can. J. Earth Sci.* 29, 260–276.
- Scott, D.J., 1997. Geology, U–Pb, and Pb–Pb geochronology of the Lake Harbour area, southern Baffin Island implications for the Paleoproterozoic tectonic evolution of northeastern Laurentia. *Can. J. Earth Sci.* 34, 140–155.
- Scott, D.J., Gauthier, G., 1996. Comparison of TIMS (U–Pb) and laser ablation microprobe ICP-MS (Pb) techniques for age determination of detrital zircons from Paleoproterozoic metasedimentary rocks from northeastern Laurentia, Canada, with tectonic implications. *Chem. Geol.* 131, 127–142.
- Speer, J.A., 1980. Zircon. In: Ribbe, P.H. (Ed.), *Orthosilicates, Reviews in Mineralogy*, vol. 5, pp. 67–112.
- Stern, R.A., Bleeker, W., 1998. Age of the world's oldest rocks refined using Canada's SHRIMP: the Acasta gneiss complex, Northwest Territories, Canada. *Geosci. Can.* 25, 27–31.
- Stewart, J.H., Gehrels, G.E., Barth, P.A., Link, P.K., Christie-Blick, N., Wrucke, C.T., 2001. Detrital zircon provenance of Mesoproterozoic to Cambrian arenites in the western United States and northwestern Mexico. *GSA Bull.* 113, 1343–1356.
- Tella, S., Heywood, W.W., Loveridge, W.D., 1985. A U–Pb age on zircon from a quartz syenite intrusion, Amer Lake map area, District of Keewatin, NWT, Current Research, Part B. Geological Survey of Canada Paper 85-1B, pp. 367–370.
- Turner, W., Richards, J., Nesbit, B., Mullenbachs, K., Biczok, J., 2001. Proterozoic low-sulfidation epithermal Au–Ag mineralization in the Mallery Lake area Nunavut, Canada, mineralium. *Deposita* 36, 442–457.
- Vennemann, T.W., Kesler, S.E., O'Neil, J.R., 1992. Stable isotope compositions of quartz pebbles and their fluid inclusions as tracers of sediment provenance: implications for gold- and uranium-bearing quartz pebble conglomerates. *Geology* 20, 837–840.
- Villeneuve, M.E., Henderson, J.R., Hrabí, R.B., Jackson, V.A., Relf, C., 1997. 2.70–2.58 Ga plutonism and volcanism in the Slave Province, District of Mackenzie, Northwest Territories. In: *Radiogenic Age and Isotope Studies, Report 10*. Geological Survey of Canada Current Research 1997-F, pp. 37–60.
- Wheeler, J.O., Hoffman, P.F., Card, K.D., Davidson, A., Sanford, B.V., Okulitch, A.V., Roest, W.R., 1996. Geological Survey of Canada Map 1860A.
- Zaleski, E., Davis, W.J., Pehrsson, S.J., Duke, N.A., L'Heureux, R., Greiner, E., 2000. Archean continental rifting recorded by orthoquartzite and bimodal komatiitic-felsic magmatism in the Woodburn Lake group, Western Churchill Province, Nunavut. *GeoCanada 2000 Meeting*, May, 2000, Calgary, Alberta. Abstract #512 (CD format).
- Zhao, G., Cawood, P.A., Wilde, S.A., Sun, M., 2002. Review of global 2.1–1.8 Ga orogens: implications for a pre-Rodinia supercontinent. *Earth Sci. Rev.* 59, 125–162.